Biomedicine & Pharmacotherapy 164 (2023) 114952

Contents lists available at ScienceDirect

Biomedicine & Pharmacotherapy

journal homepage: www.elsevier.com/locate/biopha

The novel K_V7 channel activator URO-K10 exerts enhanced pulmonary vascular effects independent of the KCNE4 regulatory subunit

Marta Villegas-Esguevillas [a,b,c,1], Suhan Cho [d,1], Alba Vera-Zambrano [a,b,c], Jae Won Kwon [b], Bianca Barreira [a,b,c], Göcken Telli [e], Jorge Navarro-Dorado [f], Daniel Morales-Cano [a,b,c], Beatriz de Olaiz [g], Laura Moreno [a,b,c], Iain Greenwood [h], Francisco Pérez-Vizcaíno [a,b,c], Sung Joon Kim [d], Belén Climent [f,*,2], Angel Cogolludo [a,b,c,2]

[a] Departamento de Farmacología, Facultad de Medicina, Universidad Complutense, Madrid, Spain
[b] Institute of Health Research Gregorio Marañón (IiSGM), Madrid, Spain
[c] CIBER Enfermedades Respiratorias (Ciberes), Madrid, Spain
[d] Department of Physiology, College of Medicine, Seoul National University, Seoul, South Korea
[e] Department of Pharmacology, Faculty of Pharmacy, Hacettepe University, Ankara, Turkey
[f] Departamento de Fisiología, Facultad de Farmacia, Universidad Complutense, Madrid, Spain
[g] Department of Thoracic Surgery, Hospital Universitario de Getafe, Getafe, Spain
[h] Vascular Biology Research Centre, Institute of Molecular and Clinical Sciences, St George's University of London, United Kingdom

ARTICLE INFO

Keywords:
K_V7 channel activator
Pulmonary hypertension
Vasodilation
KCNQ
Potassium channels
KCNE4 regulatory subunit

ABSTRACT

K_V7 channels exert a pivotal role regulating vascular tone in several vascular beds. In this context, K_V7 channel agonists represent an attractive strategy for the treatment of pulmonary arterial hypertension (PAH). Therefore, in this study, we have explored the pulmonary vascular effects of the novel K_V7 channel agonist URO-K10. Consequently, the vasodilator and electrophysiological effects of URO-K10 were tested in rat and human pulmonary arteries (PA) and PA smooth muscle cells (PASMC) using myography and patch-clamp techniques. Protein expression was also determined by Western blot. Morpholino-induced knockdown of KCNE4 was assessed in isolated PA. PASMC proliferation was measured by BrdU incorporation assay. In summary, our data show that URO-K10 is a more effective relaxant of PA than the classical K_V7 activators retigabine and flupirtine. URO-K10 enhanced K_V currents in PASMC and its electrophysiological and relaxant effects were inhibited by the K_V7 channel blocker XE991. The effects of URO-K10 were confirmed in human PA. URO-K10 also exhibited antiproliferative effects in human PASMC. Unlike retigabine and flupirtine, URO-K10-induced pulmonary vasodilation was not affected by morpholino-induced knockdown of the KCNE4 regulatory subunit. Noteworthy, the pulmonary vasodilator efficacy of this compound was considerably increased under conditions mimicking the ionic remodelling (as an *in vitro* model of PAH) and in PA from monocrotaline-induced pulmonary hypertensive rats. Taking all together, URO-K10 behaves as a KCNE4-independent K_V7 channel activator with much increased pulmonary vascular effects compared to classical K_V7 channel activators. Our study identifies a promising new drug in the context of PAH.

1. Introduction

K_V7 channels have emerged as important players in the regulation of vascular smooth muscle tone in different vascular beds. Thus, their activation causes K^+ efflux from the cell, limiting membrane depolarization and diminishing the open probability of voltage-dependent calcium channels, which reduces smooth muscle cell contraction [1–3]. Among the different K_V7 channels isoforms ($K_V7.1$–7.5), $K_V7.1$ and especially $K_V7.4$ and $K_V7.5$ channels are considered the most relevant K_V7 channels in systemic and pulmonary

* Correspondence to: Departamento de Fisiología, Facultad de Farmacia, Universidad Complutense de Madrid, 28040 Madrid, Spain.
E-mail address: bcliment@ucm.es (B. Climent).
[1] These authors contributed equally to this work.
[2] These authors share the senior authorship.

https://doi.org/10.1016/j.biopha.2023.114952
Received 21 December 2022; Received in revised form 23 May 2023; Accepted 27 May 2023
Available online 7 June 2023

vascular smooth muscle cells [1,2,4–6]. It is worth noting that recent studies have highlighted the role of K_V7 channels in the pulmonary circulation for their relevant involvement in nitric oxide (NO)-induced vasodilation [4,7].

Pulmonary arterial hypertension (PAH) is a debilitating disease defined by elevated pulmonary arterial pressure mainly due to increased vasoconstriction, pathological remodelling of the pulmonary microvasculature and thrombosis [8–10]. This pathological condition is associated with an ionic remodelling, including downregulation of different K^+ channels (such as $K_V1.5$ and TASK-1) in pulmonary artery (PA) smooth muscle cells (PASMC) leading to depolarization and ultimately contributing to increased intracellular calcium concentration, vasoconstriction, hypertrophy and proliferation [11–15]. On the other hand, K_V7 channel activity seems to be preserved in experimental models of pulmonary hypertension (PH) [5,16,17] suggesting that these channels could represent attractive pharmacological targets to limit PA vasoconstriction and proliferation in PAH. In fact, the K_V7 channel agonist flupirtine was shown to attenuate the elevated right ventricular pressure and right ventricular hypertrophy in two independent murine models of PH [16,17]. In agreement with these results, we recently found that PA vasodilation to another classical K_V7 activator, retigabine, is enhanced in the hypoxic plus Sugen 5416 PH model and suggested the upregulation of the KCNE4 regulatory subunit as a potential underlying mechanism [5]. This is a very striking result since pulmonary vasodilation to PAH-approved drugs targeting main vasodilator pathways (such as the cAMP and the cGMP pathways) appears to be greatly impaired in different models of PH [18–21]. Remarkably, activation of K_V7 channels contributes to the vascular effects induced by drugs used for the treatment of PAH such as sildenafil or riociguat [4,7]. Thus, directly targeting these channels with K_V7 channel openers might constitute a promising therapeutic strategy in the treatment of PAH [22].

K_V7 channel activity, cell localization, channel trafficking, and sensitivity to different drugs can be regulated by potassium channel subfamily E (KCNEs) regulatory subunits [3,22–24]. We have recently shown that PA have reduced expression and membrane abundance of KCNE4 [5], which is known to enhance $K_V7.4$ activity and to contribute to the vascular relaxant effects of K_V7 ligands [25,26]. This could contribute to the relatively lower vasodilatory efficacy of classical K_V7 agonists in PA compared to that observed in other arteries [5,27]. In this regard, the recently synthesised drug URO-K10 is a very potent K_V7 channel activator with EC_{50} values within the submicromolar range [28,29], and activates $K_V7.4$ and $K_V7.5$ channels independently of KCNE4 expression. Therefore, we hypothesized that URO-K10 could have augmented effects in the pulmonary circulation compared to other K_V7 channel activators, and aimed to analyse its pulmonary vascular effects in control and monocrotaline-induced pulmonary hypertension (MCT-PH) rats and in human tissues.

2. Materials and methods

2.1. Animal models

All experimental procedures utilizing animals were approved by the institutional Ethical Committee of the Universidad Complutense de Madrid (Spain), the regional Committee for Laboratory Animals Welfare (Comunidad de Madrid, Ref. number PROEX-301/16) and the Institutional Animal Care and Use Committee of Seoul National University (approval number: SNU-190408–3) and are reported in accordance with the ARRIVE guidelines. The animals were cared according to the Directive 2010/63/EU of the European Parliament on the protection of animals used for scientific purpose.

6–8-week-old male Wistar and Sprague-Dawley rats (300 ± 20 gr) were obtained from Envigo (Barcelona, Spain) and Koateg (Pyeongtaek-si, South Korea), respectively. The animals were housed at the Institutions animal care facilities and kept in an enriched environment with free access to food and water, maintained at 24 °C under a 12:12 h light/dark cycle. Animal experiments were designed to have groups of equal size using randomized and blinded analysis. In some instance, however, group sizes were unequal due to unexpected loss of animals while conducting the procedures. Monocrotaline (Sigma, St. Louis, MO, USA) was dissolved in 2 mL of 1 mol L^{-1} HCl and adjusted to pH 7.4 using 2 mol L^{-1} NaOH solution. This aqueous solution was diluted to 17 mL with distilled water. Sprague-Dawley rats were randomly assigned and treated with a single intraperitoneal injection of monocrotaline (60 mg kg^{-1}) to induce PH or an appropriate amount of saline. After 21 days, both the MCT-PH rats and the age-matched controls were sacrificed for further analysis, after measuring their body weight.

2.2. Human Samples

Human PA and PASMC were isolated from lung samples obtained from 13 non-PAH patients (6 men, 8 women, mean age 70.0 ± 2 years) who underwent lobectomy for localized lung cancer in Hospital de Getafe (Madrid, Spain). The Human Research Ethics Committee of the Hospital Universitario de Getafe (Madrid, Spain) approved the use, after informed consent, of lung tissue discarded by pathologists following thoracic surgery (Ref. A04/16).

2.3. Tissue collection and cell isolation

On the experiment day rats were sacrificed by CO_2 inhalation. Rat lungs, human lung samples and mesenteric beds were isolated and placed in chilled (4 °C) Krebs solution of the following composition (in mmol L^{-1}): NaCl 119, KCl 4.7, KH_2PO_4 1.2, $MgSO_4$ 1.2, $CaCl_2$ 2, glucose 11 and sodium bicarbonate 11; pH7.4. Lungs from Sprague-Dawley were isolated and immersed in Tyrode's solution (in mmol L^{-1}): NaCl 140, KCl 5.4, NaH_2PO_4 0.33, HEPES 10, glucose 10, $CaCl_2$ 1.8 and $MgCl_2$ 1, pH 7.4 was adjusted with NaOH. Isolation of human PA and rat PA and mesenteric arteries (MA) was performed as previously described [27,30]. Freshly isolated rat and human PASMC were obtained by enzymatic digestion, as described previously [31]. Briefly, PA were dissected in Ca^{2+}-free physiological salt solution (Ca^{2+}-free PPS) composed of (in mmol L^{-1}): NaCl 130, KCl 5, $MgCl_2$ 1.2, glucose 10, and HEPES 10 (adjusting to pH 7.3 with NaOH). For isolation of PASMC, PA were cut longitudinally and incubated in Ca^{2+}-free PPS containing (in mg mL^{-1}): papain 1, dithiothreitol 0.8, and albumin 0.7 for 10–20 min. After vigorous agitation using a smooth wide-tipped pipette, the tissue was dissociated and a PASMC suspension was obtained, which was stored at 4 °C.

PASMC from MCT-PH rats were isolated as follows. Briefly, PA were cut to open and digested with first digestion medium (nominal Ca^{2+}-free Tyrode's solution containing 1 mg mL^{-1} papain) for 10–15 min. The fragmented tissues were collected and incubated with second digestion medium (nominal Ca^{2+}-free Tyrode's solution containing 3 mg mL^{-1} collagenase) for another 10 min. Both digestion media contained bovine serum albumin (1 mg mL^{-1}) and dithiothreitol (1 mg mL^{-1}). The digested tissues were suspended with a polished Pasteur pipette in K^+-rich solution (in mmol L^{-1}): KOH 70, L-glutamate 50, KCl 55, taurine 20, KH_2PO_4 20, $MgCl_2$ 3, glucose 20, HEPES 10 and EGTA 0.5, adjusted to pH 7.3 with KOH, to dissociate into single cell for the further analysis.

2.4. Experimental procedures for the vascular reactivity studies

Rat PA and MA and human PA were mounted in a wire myograph (model 610 M, Danish Myo Technology, Aarhus, Denmark) with Krebs solution at 37 °C and bubbled with aerobic gas (CO_2: 5%, N_2: 74%, O_2: 21%) for the PA and carbogen gas (O_2: 95%, CO_2: 5%) (Air Products - Carbides) for the MA. The relationship between passive wall tension and internal circumference was determined for each individual artery and from this, the internal circumference, L30 (for PA) and L100 (for MA), corresponding to a transmural pressure of 30 mmHg and 100 mmHg, respectively, for a relaxed vessel *in situ* was calculated. The arteries were

set to an internal diameter L1 equal to 0.9 times L30 or L100 (L1 = 0.9 x L30 for PA and L1 = 0.9 x L100 for MA), since force development in arteries is close to maximal at this internal lumen diameter [32]. The transmural pressure of 30 mmHg selected for pulmonary arteries was based on previous studies [33,34]. Arteries were first stimulated by raising the K^+ concentration of the buffer (to 80 mmol L^{-1}) in exchange for Na^+. Next, vessels were washed three times and allowed to recover before a new stimulation. The vasodilator responses to URO-K10 (0.0001–3 μmol L^{-1}), retigabine (0.01–30 μmol L^{-1}) and flupirtine (0.01–30 μmol L^{-1}) were assessed in arteries precontracted with the thromboxane A_2 analogue U46619 (PA at 0.1 μmol L^{-1} and MA at 0.3 μmol L^{-1}) or serotonin (10 μmol L^{-1}) [35,36]. In some experiments, the effects of URO-K10 were tested in arteries incubated for 15 min with the K_V7 channel inhibitor XE991 (3 or 10 μmol L^{-1}) or with the combination of the $K_V1.5$ channel inhibitor diphenylphosphine oxide-1 (DPO-1, 1 μmol L^{-1}) and the TASK-1 channel inhibitor ML365 (1 μmol L^{-1}), before the challenge to the contractile agent.

2.5. Human PASMC proliferation

Human PASMC proliferation was measured using the colorimetric assay based on the incorporation of 5-bromo-2-deoxyuridine (BrdU). Cells were grown in a flask with supplemented smooth muscle cell growth medium (C22062; PromoCell, Heidelberg, Germany) and kept in an incubator at 37 °C, 99% humidity and 5% CO_2. Human PASMC already seeded in 96-well plate (5000 cells/well) were growth arrested by an exposure for 24 h in 0.1% FBS medium and then exposed to smooth muscle cell growth medium containing 5% FBS for 24 h to stimulate growth. To characterize the possible antiproliferative effect of URO-K10, human PASMC were treated with different concentrations: 0.01, 0.1 and 1 μmol L^{-1} in 5% FBS medium. In another set of experiments and to elucidate the mechanism of action of URO-K10 on proliferation, we tested the effect of XE991 10 μmol L^{-1} in the presence and in the absence of URO-K10 (1 μmol L^{-1}) in medium containing 5% FBS. During the final 6 h of the 24 h treatment, BrdU was added to the cells. The absorbance was measured on a spectrophotometric plate reader (EZ Read 400 Microplate Reader, Biochrom) at a dual wavelength of 450–620 nm [37]. Proliferation analyses of cultured human PASMC were carried out in triplicate for each sample. Data are expressed as percentage of proliferation induced by FBS 5%. The data group size in this set of experiments is 3–4 data due to the very limited amount of human PASMC.

2.6. Electrophysiological studies

Membrane currents were recorded with the Axopatch 200B amplifier and with Digidata 1322 A (Axon Instruments, Burlingame, CA, USA) or Digidata-1440A (Molecular Devices, San Jose, CA, USA) using the ruptured patch configuration of the whole cell patch-clamp technique, as previously described [4,38–40]. Micropipettes were created from borosilicate glass capillaries with a programmable horizontal pipette puller and polisher (Zeitz DMZ Puller, AutoMate Scientific).

For the whole cell recording, freshly isolated PASMC were either superfused with an external Ca^{2+}-free PPS (see above) or an external solution of the following composition (in mmol L^{-1}): NaCl 140, KCl 5, HEPES 10, $CaCl_2$ 2, $MgCl_2$ 1, glucose 5, mannitol 20, and pH 7.4. Pipettes were filled with a solution of the following composition (in mmol L^{-1}): KCl 140, HEPES 10, Tris-GTP 0.2, Na-ATP 4, EGTA 10 with 100 nmol L^{-1} free Ca^{2+}, and pH 7.2.

K_V currents were evoked after the application of 200 ms depolarizing pulses from + 60 mV to − 80 mV in 10 mV decreasing steps or by depolarizing ramp pulses from − 100–40 mV for 3 s, from a starting potential of − 80 mV. The electrophysiological effects of URO-K10 (0.3 or 1 μmol L^{-1}) were tested until they reached steady state (normally 7–10 min). In some experiments we checked the effect of URO-K10 in PASMC after 10 min exposure to DPO-1 (1 μmol L^{-1}) plus ML365 (1 μmol L^{-1}). These two protocols were also performed after incubation with XE991 (10 μmol L^{-1}) for approximately 20 min. Currents were normalized for cell capacitance and expressed in pA pF^{-1}. Membrane potential was recorded under the current-clamp mode. Only cells with acceptable values of leak current (less than 50 pA) and series resistance (Rs, in the range of 5–30 MΩ) were follow-up. Rs and leak current values were checked regularly during the experiment, before and after the addition of a given drug. Recordings with evidence of current instability or membrane resealing were discarded as well as those where the leak currents or series resistance were changed by more than 20%.

2.7. Molecular interference with morpholino

The morpholino mechanism of action is based on a steric block mechanism to a messenger RNA, which inhibits specifically the transcription of the desired gene. Control morpholino has five bases altered from the targeted sequence, which offers increased assurance that the effects observed are not the result of off-target modulation [41,42]. Compared to other knockdown systems employed, morpholinos have excellent anti-sense properties, because of the increased complementarity with their target mRNA and they are also free of the widespread off-target expression modulation often observed in other knockdown systems [41,42]. Consequently, KNCE4 was knocked down in isolated PA using specific morpholino oligos. The KCNE4 morpholino was designed to block translation initiation in the cytosol by targeting the 5 ́untranslated region through the first 25 bases of coding sequence as previously reported (Jepps et al., 2015). Morpholino or a standard control oligonucleotides (Gene Tools Inc., Philomath, OR, USA) were mixed with Lipofectamine RNAiMAX (Life Technologies Corp) and diluted in Opti-MEM containing antibiotic 1% and left at room temperature for 2 h. Afterwards, morpholino and control mixes were incubated with the Lipofectamine one for 15 min at room temperature. Further dilution of the mixes was prepared in Opti-MEM plus antibiotic and isolated PA were placed in this solution at 37 °C for 40 h. This incubation period was chosen to allow sufficient time to repress the targeted gene expression without severely affecting the functionality of the PA [43,44], as incubations longer than 48 h can markedly alter pulmonary vascular reactivity and sensitivity to potassium channel modulators [45]. Successful knockdown of the protein with the targeted morpholino was assessed by western blotting and compared with the respective control morpholino.

2.8. Western blot analysis

Pulmonary arteries were dissected from rat lungs (n = 11) and snap frozen in liquid nitrogen and kept in − 80 °C. Samples were homogenized in RIPA Buffer (Thermo Scientific, USA) with protease inhibitors (Roche, Switzerland) and centrifuged for 20 min at 12.000g at 4 °C as previously described [46]. Protein content was determined by Bio-Rad DC Protein Assay Kit (Bio-Rad, Hercules, USA) and equal amounts of proteins (20 μg) were loaded and subjected to electrophoresis on a SDS-PAGE (12%) followed by a transference to a PVDF membrane (Bio-Rad). Protein expression was quantified using primary antibodies anti-KCNQ5 (Alomone, Israel, 1:200 dilution, Cat #: APC-155), anti-KCNQ4 (Santa Cruz, USA, 1:200 dilution, Cat #: Sc-50417), anti--KCNE4 (Atlas, Sweden, 1: 200 dilution, Cat #: HPA011420), anti-vinculin (Santa Cruz, USA, 1:500 dilution, Cat#: Sc-25336), and horseradish peroxidase conjugated secondary goat anti-mouse and anti-rabbit antibodies (Santa Cruz Biotech, USA, 1:10.000 dilution). Antibody specificity has been previously tested according to BJP guidelines [47] either by using protein lysates from HEK293 cells transfected with Kv7.4 or KCNE4 and non-transfected controls [25,48] or by using controls in the absence of the primary antibody for the $K_V7.5$ [49,50]. Antibody binding was detected by an ECL system (Amersham PharmaciaBiotech, Amersham, UK).

2.9. Drugs

Drugs and reagents were obtained from Sigma-Aldrich Quimica (Madrid, Spain), except URO-K10 that was provided by Sundia MediTech Company (Sanghai, China) based on reaction scheme suggested by Seefeld et al. [28]. Stock solutions of URO-K10, flupirtine, retigabine and U46619 were dissolved in DMSO and then further diluted in distilled water. The final volume of DMSO or ethanol never exceeded 0.01% in organ baths and did not affect smooth muscle tone in control experiments. All the other drugs were dissolved in distilled water.

2.10. Data presentation and Statistical analysis

In the myography experiments, the vasodilatory responses are expressed as the percent reversal of the previous constriction with either U46619 or serotonin in each artery. Data are expressed as mean ± standard error of the mean (SEM) of n measurements where n identifies the number of animals or patients. Individual cumulative concentration response curves were fitted to a logistic equation. The maximal relaxant response (Emax) was expressed as percentage of inhibition of the contraction induced by the vasoconstrictor and the concentration of agonist that gives a response of a 50% of the Emax was calculated from this equation and expressed as pD2 = -log EC50. When maximal relaxant response could not be reached, the drug concentration exhibiting 30% relaxation was calculated from the fitted concentration-response curves and expressed as negative log molar (-log IC_{30} or pIC_{30}). The differences between means were analysed using a two-way ANOVA, one-way ANOVA, paired or unpaired Student's *t*-test as appropriate. In the myography experiments, after the two-way ANOVA analysis was performed, the analyses of area under the curve (AUC) were used to represent the difference in concentration response relaxation curves whenever a comparison with more than 2 different groups was needed. The level of significance was set at $P < 0.05$. All calculations were made using a standard software package (Prism 8.0.2, GraphPad, CA, USA). For electrophysiological experiments pClamp version 9 software (Axon Instruments) was used for data acquisition and analysis. For protein expression studies, western blots were imaged using Image Studio Lite 4.0 software (LI-COR Biosciences, Germany). Relative intensity for each protein was determined by comparison with the intensity of vinculin staining as a loading control.

3. Results

3.1. URO-K10 induces much stronger pulmonary vasodilation compared to classical K_V7 activators

We first tested the pulmonary vasodilator effects of URO-K10 (0.0001 – 3 μmol L^{-1}) and the classical K_V7 activators retigabine and flupirtine (0.01 – 30 μmol L^{-1}) in U46619-stimulated PA (Fig. 1A-B). Unlike retigabine, URO-K10 was able to induce a marked vasodilator response in PA yielding Emax and pD2 values of 58 ± 5% and 7.29 ± 0.08, respectively. However, flupirtine-induced vasodilation was

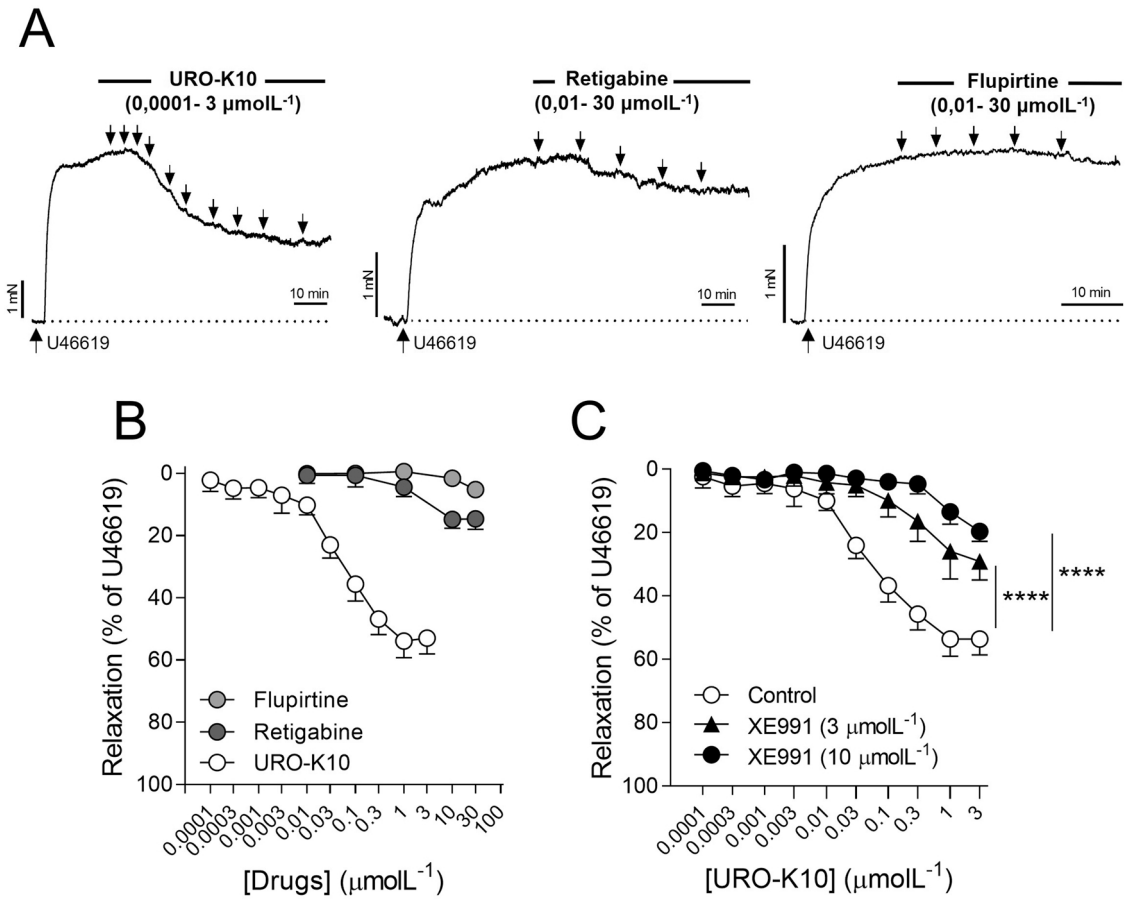

Fig. 1. URO-K10 produces more potent and efficient pulmonary vasorelaxation than classical K_V7 channel activators. (a) Original recordings and (b) averaged concentration-dependent relaxant effects of URO-K10, retigabine and flupirtine in U46619-stimulated PA. Points represent mean ± SEM of n = 9, n = 9 and n = 5 for URO-K10, retigabine and flupirtine, respectively. (c) Averaged concentration-dependent relaxation effects to URO-K10 in the absence and in the presence of the K_V7 channel inhibitor XE991 (3 or 10 μmol L^{-1}). Points represent mean ± SEM of n = 9, n = 5 and n = 5 for URO-K10, + XE991 3 μmol L^{-1}, and + XE991 10 μmol L^{-1}, respectively. Results are expressed as a percentage of the contraction induced by U46619 (0.1 μmol L^{-1}). Significant differences from controls were analyzed using two-way ANOVA. * ** * $P < 0.0001$ *vs* control.

comparable to that observed following the addition of the vehicle (supplementary Figure 1). The pre-constrictions levels to U46619 in PA were 81 ± 12, 76 ± 3 and 96 ± 12 for URO-K10-, retigabine- and flupirtine-induced relaxation, respectively (n = 9, n = 7 and n = 5, $P > 0.05$, one-way ANOVA). Of note, URO-K10-induced vasorelaxation was inhibited in a concentration-dependent manner by the K_V7 channel inhibitor XE991, confirming the role of K_V7 channels as its main underlying vasodilator mechanism (Fig. 1 C). Moreover, the low relaxation remaining after XE991 was comparable to that observed following the addition of vehicle (supplementary Figure 2 A). Next, we tested the effect of URO-K10 in the presence of the BK_{Ca} blocker, iberiotoxin (100 nmol L^{-1}), which did not affect URO-K10-induced relaxation (supplementary Figure 2B). The pre-constrictions levels to U46619 in Fig. 1 C were 81 ± 12%, 81 ± 6% and 82 ± 8% of the contraction induced by KCl (80 mmol L^{-1}) for URO-K10, URO-K10 in the presence of XE991 3 μmol L^{-1} and URO-K10 in the presence of XE991 10 μmol L^{-1}, respectively (n = 9, n = 5 and n = 5, $P > 0.05$, one-way ANOVA). The pre-constrictions levels to U46619 (% of KCl) in supplementary Figure 2 A were 78 ± 8% and 85 ± 3% for URO-K10 vehicle (n = 5 and n = 5, P > 0.05, unpaired *t*-test), respectively, and in supplementary Figure 2B were 79 ± 14% and 72 ± 4% (% of KCl) for URO-K10 and URO-K10 in the presence of iberiotoxin (n = 7 and n = 6, $P > 0.05$, unpaired *t*-test),

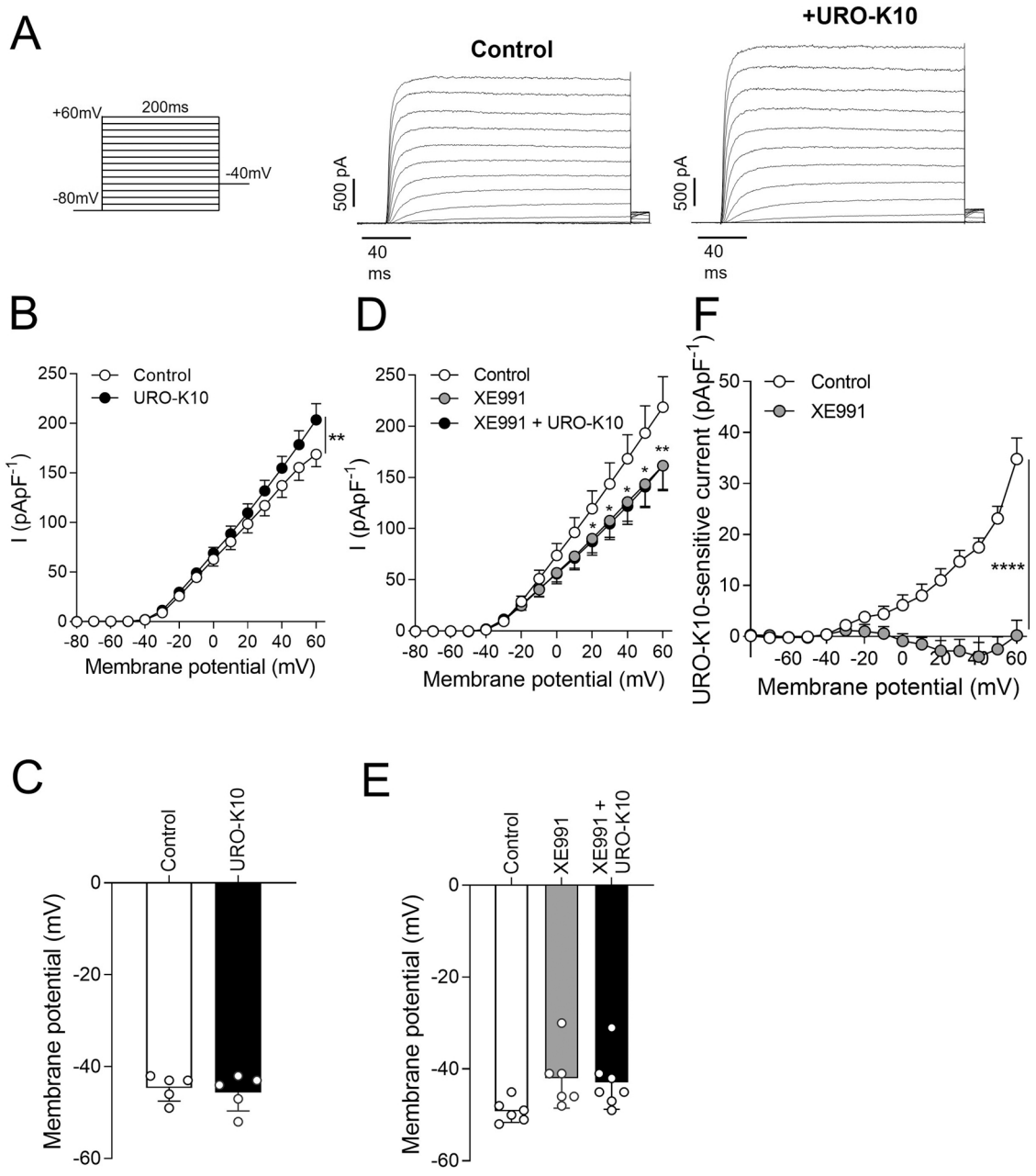

Fig. 2. . URO-K10 increases the K_V current by activating K_V7 channels in freshly isolated PASMC from control rats. (a) Representative K^+ current traces and (b) K^+ current-voltage relationships measured at the end of the depolarizing pulses in the absence and in the presence of URO-K10 (0.3 μmol L^{-1}). (c) Mean values of the resting membrane potential in the absence and in the presence of URO-K10 (n = 5, $P > 0.05$, paired *t*-test). (d) K^+ current-voltage relationships measured at the end of the depolarizing pulses in the absence and presence of XE911 (10 μmol L^{-1}) and XE911 + URO-K10 (n = 6, $P < 0.001$ control *vs* XE991, two-way ANOVA followed by a Bonferroni post-test). (e) Mean values of the resting membrane potential in the absence and in the presence of XE911 (10 μmol L^{-1}) and XE911 + URO-K10 (n = 6, $P > 0.05$, one-way ANOVA). (f) URO-K10-sensitive current in control and in the presence of XE991 (n = 6, **** <0.0001. Data were analyzed by two-way ANOVA).

respectively.

URO-K10 produced a greater vasodilation in MA (Emax= 107 ± 3%, pD_2: 8.50 ± 0.3, n = 5) (supplementary Figure 3) compared to PA ($P < 0.0001$, for Emax and $P > 0.05$ for pD_2, un-paired t-test, n = 9 and n = 5 for PA and MA, respectively), as observed previously for other K_V7 activators [5,27]. Pre-constrictions levels to U46619 in Suppl. Fig. 3 were 159 ± 27% and 156 ± 21% of KPSS-induced contraction in the absence and in the presence of DPO and ML365, respectively ($P > 0.05$, paired t-test, n = 5). Like other K_V7 activators, the relaxation to URO-K10 in MA was inhibited by XE991 confirming the role of K_V7 channels (supplementary Figure 3).

In line with our vascular function data, we observed that URO-K10 increased outward K_V currents in isolated PASMC using the whole-cell patch-clamp configuration (Fig. 2A-B) and such an increase was abolished in the presence of XE991, confirming that URO-K10 induced K_V7 channels activation (Fig. 2D). The URO-K10-sensitive K_V current was calculated by subtracting the current in the presence of URO-K10 to that in the absence of the drug and was evident at membrane potentials more positive than − 40 mV (Fig. 2 F). In addition, the URO-K10-sensitive K_V current was abolished in the presence of XE991 (Fig. 2 F) and application of the vehicle of URO-K10 (DMSO) did not elicit any outward current (supplementary Figure 4 A). In fact, the resting membrane potential of PASMC, which was about − 45 mV, was not significantly altered by URO-K10 nor by XE991 (Fig. 2 C and E). Moreover, application of the vehicle of URO-K10 (DMSO) did not elicit any outward current nor any change in membrane potential (Suppl. Fig. 4B).

3.2. URO-K10 causes relaxation, increases K_V currents and causes an antiproliferative effects in human PA

In the next set of experiments, we evaluated the effects of URO-K10 in human samples. Importantly, we found that, compared to retigabine, URO-K10 behaved as a very potent and efficient vasodilator in human PA (pIC_{30} = 7.0 ± 0.2 *vs* 4.4 ± 0.3; $P < 0.0001$, unpaired *t*-test) (Fig. 3A-B). Pre-constrictions levels to U46619 in Fig. 3B were 250 ± 30% and 224 ± 36% for URO-K10 and retigabine (n = 6 and n = 5, $P > 0.05$, unpaired *t*-test), respectively. As observed in rat PASMC, URO-K10-induced relaxation was markedly inhibited in the presence of XE991 (supplementary Figure 5 A) and URO-K10 increased the K_V current density in freshly isolated human PASMC (Fig. 3 C-D), without altering resting membrane potential (Fig. 3E). In addition, control experiments with application of the vehicle alone (DMSO) produced a

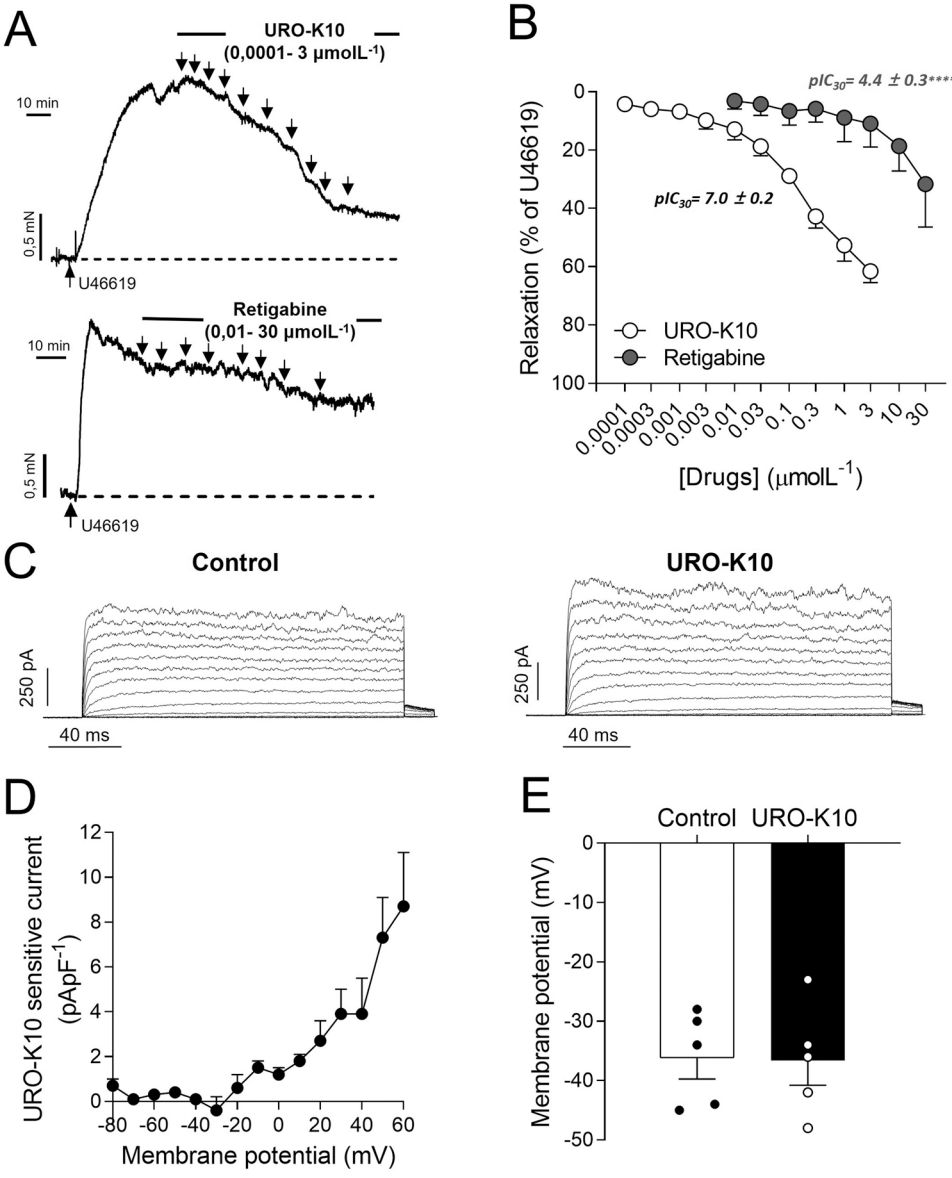

Fig. 3. . URO-K10 causes vasodilatation and increases K_V currents in freshly isolated PA and PASMC from human samples. (a) Isometric tension recordings showing the effects of increasing concentrations of URO-K10 (0.0001–3 µmol L^{-1}) and retigabine (0.01 −30 µmol L^{-1}) on human PA contracted with U46619 (0.1 µmol L^{-1}). (b) Averaged concentration-dependent relaxant effects to URO-K10 and retigabine on human PA. Points represent mean ± SEM (n = 6 and 4 for URO-K10 and retigabine, respectively). (c) Representative K^+ current traces recorded in human PASMC in the absence and in the presence of URO-K10. (d) URO-K10-sensitive current measured at the end of the depolarizing pulses obtained by subtracting the K^+ current in the presence of URO-K10 from the current in the absence of the drug. (e) Mean values of the hPASMC resting membrane potential in the absence and in the presence of URO-K10 (n = 5, $P > 0.05$, paired *t*-test).

negligible vasodilator effect which was statistically different than the relaxation induced by retigabine (supplementary Figure 5B). Moreover, we tested whether URO-K10 had antiproliferative effects in human PASMC and observed that this compound at 1 μmolL^{-1} inhibited PASMC proliferation (Fig. 4). In addition, our preliminary data in supplementary Figure 6 indicate that in the presence of XE991 the antiproliferative effect of URO-K10 is attenuated (supplementary Figure 6, preliminary data due to limited availability of human tissue, n = 3), however, it also must be noted that XE991 *per se* attenuated the BrdU signal. Altogether our data indicate that URO-K10 has very potent vasodilator and antiproliferative effects in rat and human PA.

3.3. URO-K10-induced relaxation in PA is independent of the KCNE4 ancillary subunit

Next, we explored possible mechanistic differences between URO-K10 and classical K_V7 activators that could explain the significantly different functional behaviour and focused on the KCNE4 subunit. This regulatory subunit is crucial for $K_V7.4$ translocation to smooth muscle cell membranes [25,51] and has been implicated in relaxant responses to the $K_V7.2$–7.5 activator S-1 in mesenteric arteries [25,26]. In contrast, KCNE4 was shown to impair URO-K10 enhancement of $K_V7.4$ currents [29]. Thus, we treated PA with morpholinos designed to target KCNE4 as previously reported [25]. We first confirmed by Western blot analysis that KCNE4-targeted morpholino reduced KCNE4 expression in PA by around 50% (Fig. 5A-B). Interestingly, treatment with KCNE4-targeted morpholino also led to a slight but significant reduction of $K_V7.4$ (Fig. 5C-D), but not $K_V7.5$ (Fig. 5E-F), channel expression. Then, we compared the vasodilator effects of URO-K10 and retigabine in PA transfected with KCNE4-targeted *vs* non-targeted morpholinos. Interestingly, we observed that URO-K10-induced relaxation was unaffected (Fig. 6A-B), while the vasodilation induced by retigabine (Fig. 6D-E) was reduced by KCNE4 knockdown. In addition, control experiments with application of the vehicle alone (DMSO) produced a negligible vasodilator effect that was statistically different than the relaxation induced by retigabine (Fig. 6E and supplementary Figure 8). Concentration-response relationships to U46619 for control cultured vessels were performed and the dose of 0.1 μmol L^{-1} induced a constriction level of 91 ± 1% of maximal U46619 contraction (n = 5).

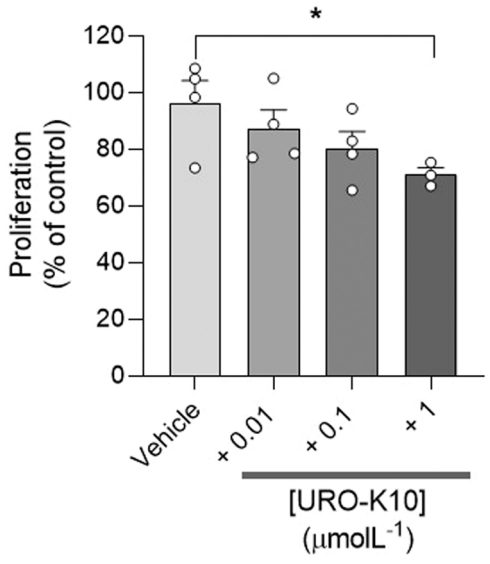

Fig. 4. . Antiproliferative effects of URO-K10 in human PASMC. (a) Concentration-dependent inhibition of BrdU incorporation induced by URO-K10 in human PASMC. Data are expressed as percentage of proliferation induced by FBS 5% (n = 4, * $P < 0.05$ *vs* vehicle, one-way ANOVA followed by a Dunnet test).

Pre-constriction levels, expressed as a percentage of the KPSS-induced maximal contraction, were similar in control and KCNE4-targeted vessels (Fig. 6B: 125 ± 25% *vs* 122 ± 11%, n = 5; Fig. 6E: 131 ± 19% *vs* 130 ± 9, and n = 5, $P > 0.05$, paired *t*-test). We also tested the impact of KCNE4 downregulation on flupirtine-induced vasodilation in serotonin-stimulated PA, a vasoconstrictor less resistant to vasodilators than U46619. Under these conditions flupirtine induced a greater relaxant response that was significantly attenuated in *KCNE4*-targeted PA (Supplementary Figure 9A-B). Pre-constriction levels from Suppl. Fig. 8B were also similar in control and KCNE4-targeted vessels (130 ± 20% *vs* 134 ± 49% in control and KCNE4-targeted PA, respectively, $P > 0.05$, paired *t*-test, n = 5). Moreover, XE991 inhibited the relaxation induced by all the drugs in PA transfected with non-targeted morpholinos. Interestingly, retigabine- and flupirtine-induced relaxation was inhibited by XE991 in control but not in morpholino KCNE4-targeted PA (Fig. 6 C and F, Suppl. Figure 9C-D). Taking altogether our data indicate that, unlike retigabine and flupirtine, URO-K10 exerts pulmonary vasodilator effects *via* K_V7 channel activation independently of KCNE4.

3.4. Enhanced responses to URO-K10 in the presence of TASK-1 and $K_V1.5$ inhibitors

Since downregulation of K^+ channels, especially TASK-1 and $K_V1.5$, is a common hallmark of PAH [37,52–58], we then tested the effect of URO-K10 under conditions mimicking this ionic channel remodelling characteristic of the disease. In this regard, we evaluated the pulmonary vascular effects of URO-K10 in the presence of the $K_V1.5$ and TASK-1 channel inhibitors DPO-1 (1 μmol L^{-1}) and ML365 (1 μmol L^{-1}), respectively. As shown in Fig. 7, URO-K10 induced a much greater relaxation under these conditions compared to arteries unexposed to these potassium inhibitors (Fig. 7 A and B). On the other hand, the inhibition of TASK-1 and $K_V1.5$ channels did not affect the URO-K10-induced relaxation in MA (Supplementary Figure 3 A). Pre-constrictions levels to U46619 in MA from Suppl. Fig. 3 were equal either in the absence or in the presence of TASK-1 and $K_V1.5$ channels inhibitors (159 ± 27 and 156 ± 21, respectively ($P > 0.05$, paired *t*-test, n = 5).

As expected, the total K^+ current amplitude was markedly diminished in PASMC treated with the DPO-1 + ML365 combination (compare recordings in Fig. 2 A and 7 C). Interestingly, further addition of URO-K10 caused a significant increase in these currents (Fig. 7 C and D). The URO-K10-sensitive current in PASMC treated with ML365 + DPO-1 was comparable to that observed under control conditions ($p > 0.05$, two-way ANOVA, n = 5 and n = 6, Fig. 7E). In addition, we have tested the effects of XE991 on URO-K10-induced current in the presence of DPO-1 + ML365. Our data shows that the current induced by URO-K10 in the presence of DPO-1 + ML365 is prevented by XE991, indicating that under these conditions URO-K10 increases the current also *via* K_V7 channel activation. Moreover, the URO-K10-sensitive current in PASMC treated with ML365 + DPO-1 was abolished in the presence of XE991 (supplementary Figure 10). Remarkably, in the presence of ML365 + DPO-1, which led to a marked membrane depolarization, a clear repolarizing effect was observed following the addition of URO-K10 (Fig. 7 F and G).

3.5. Augmented responses to URO-K10 in PA from PH animals

Finally, we studied the effects of URO-K10 in PA derived from MCT-PH animals. Of note, we found that the vasodilator efficacy to URO-K10 was significantly stronger in PA from MCT-PH rats compared to those from control animals (Emax= 60 ± 7% *vs* 102 ± 10%, $P < 0.05$, unpaired nested *t*-test; and pD_2: 6.31 ± 0.06 *vs* 6.48 ± 0.10, $P > 0.05$, unpaired nested *t*-test, 12 arteries from n = 3 animals in control and 10 arteries from n = 3 animals for the MCT group) (Fig. 8 A and B). Pre-constriction levels to U46619, expressed as a percentage of the KPSS-induced maximal contraction, were 124 ± 19% and 106 ± 6% for the

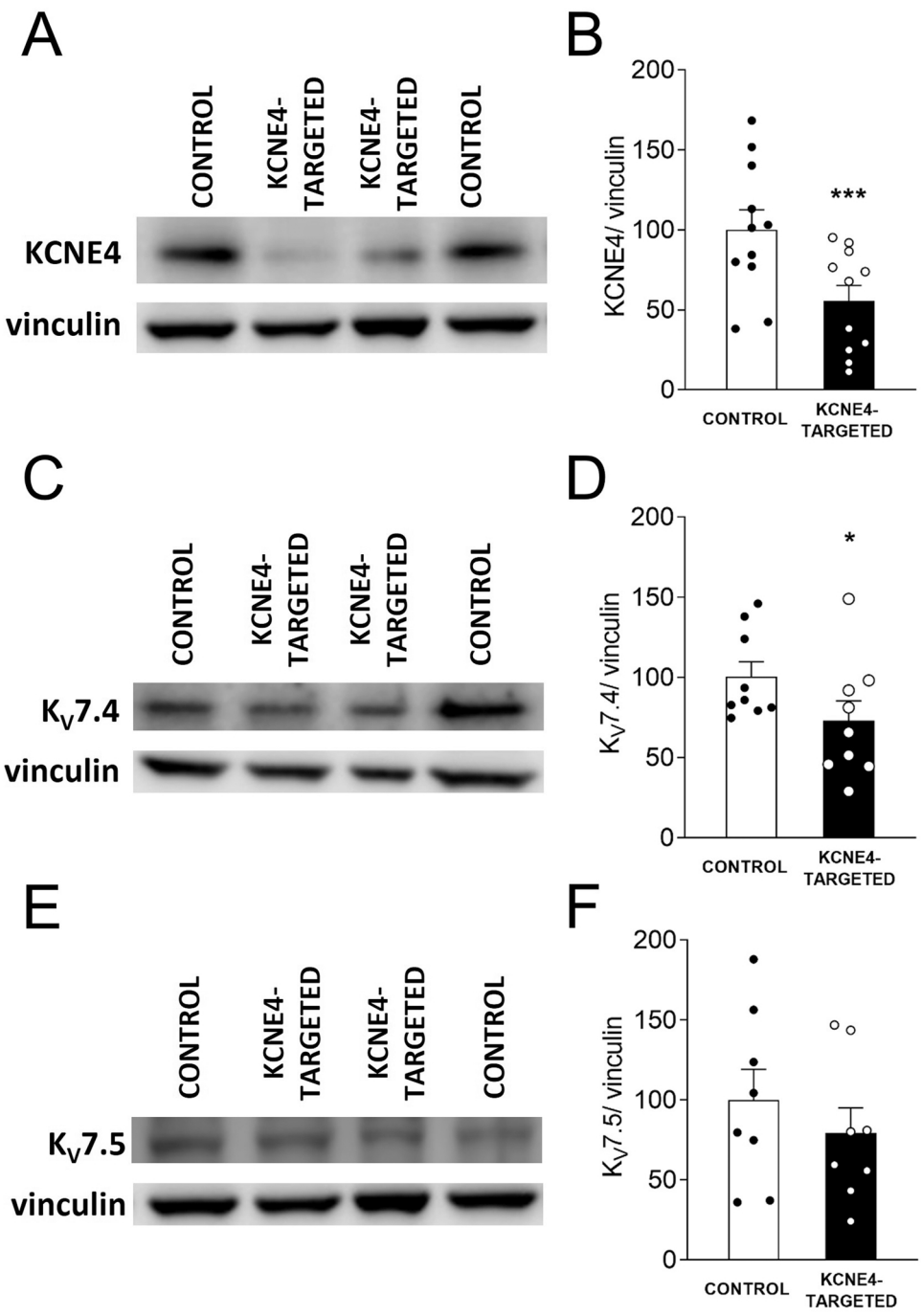

Fig. 5. . KCNE4-targeted morpholino effectively reduces KCNE4 and partially decreases K_V7.4 channel protein expression in PA. Representative Western blot and mean data of KCNE4 (a and b), K_V7.4 channel (c and d) and K_V7.5 channel (e and f) expression in PA transfected with either a KCNE4-targeted or the respective control morpholino. Protein expression was normalized by vinculin expression. Data are shown as means ± SEM of PA from n = 8, 9 and 11 animals for K_V7.5 channel, K_V7.4 channel and KCNE4 subunit, respectively. Significant differences were analyzed by using paired *t*-test. * $P < 0.05$ and * ** $P < 0.001$ *vs* control morpholino.

control and MCT group (n = 3 and n = 3, respectively). Moreover, we studied the electrophysiological effects of URO-K10 in PASMC from PH rats by applying depolarizing pulses from − 100 to + 40 mV. Cells were subsequently perfused with control external solution (a), URO-K10 (1 μmol L^{-1}) (b), and with URO-K10 (1 μmol L^{-1}) + XE991 (30 μmol L^{-1}) (c). Fig. 8C-D shows the K_V7 current and the K_V7 current after URO-K10 calculated by subtracting the currents at (a)-(c) and at (b)-(c), respectively, in PASMC from control (Fig. 8 C) or MCT-PH (Fig. 8D) rats. As can be seen, URO-K10 greatly increased the K_V7 current in both cell types. Of note, the K_V7 current after URO-K10 was remarkably higher in cells from PH compared to control animals (Fig. 7E).

4. Discussion

Herein, we show that URO-K10, through K_V7 channel activation, increases K_V currents in PASMC and exerts a very potent and efficient pulmonary vasodilation in rat PA compared to other K_V7 channel activators. The URO-K10-induced vascular effects are also confirmed in human PA and remarkably, this drug caused antiproliferative effects in human PASMC. Interestingly, while the auxiliary subunit KCNE4 is necessary for retigabine and flupirtine-induced vascular effects, this does not apply for URO-K10. In addition, URO-K10-induced vasodilation was augmented under conditions mimicking the ionic remodelling associated with PAH. Finally, URO-K10-induced enhanced vascular responses and K_V currents in PA and PASMC from the MCT-PH rats. Hence, our results indicate that, unlike retigabine and flupirtine, URO-K10

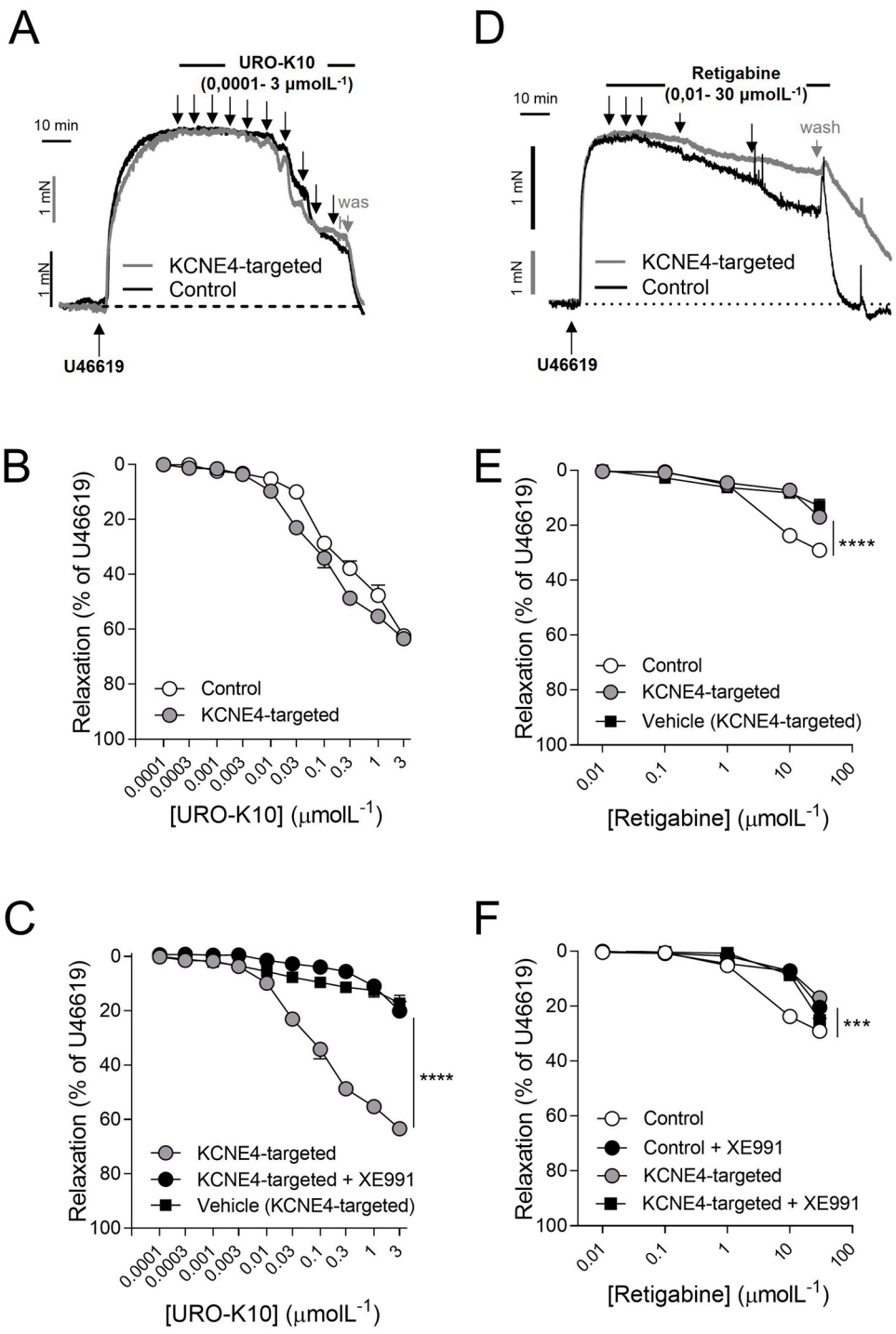

Fig. 6. . KCNE4 knockdown attenuates retigabine- but not URO-K10-induced pulmonary vasodilatation. Original recordings (a and d) and averaged values (b-f) of the concentration-dependent relaxation induced by URO-K10 (0.0001 – 3 µmol L^{-1}) and retigabine (0.01 – 30 µmol L^{-1}) and vehicle, respectively, in rat PA transfected with either a KCNE4-targeted or the respective control morpholino in the presence and in the absence of XE991 (10 µmol L^{-1}). (c) Points represent mean ± SEM of n = 5–8. Significant differences were analyzed by using two-way ANOVA. * ** $P < 0.001$, * ** * $P < 0.0001$ *vs* control morpholino and * ** $P < 0.001$ *vs* KCNE4 targeted.

behaves as a KCNE4-independent K_V7 channel activator with a marked pulmonary vascular response.

Since K_V7 channels are important players in the regulation of vascular smooth muscle tone, targeting these channels represents an attractive pharmacological tool for the treatment of smooth muscle-associated disorders including those targeting the lung [1,3,22,59–61]. The $K_V7.2$-$K_V7.5$ channel activators flupirtine and retigabine, commercialized as analgesic and anticonvulsant drugs respectively, were withdrawn from the market due to undesirable side effects [62–64]. In this regard, we have examined the pulmonary vascular effects of URO-K10, a novel K_V7 channel opener which enhances K^+ currents in $K_V7.4$- and $K_V7.5$ channel-expressing HEK293 cells and relaxes mesenteric arteries at low concentration [29]. We show that URO-K10 was a highly effective relaxant of PA from rats and humans. The relaxant effects of URO-K10 were abrogated by the pan-K_V7 channel blocker XE991 but not affected by the BK_{Ca} channel inhibitor IbTx. This is consistent with the idea that K_V7 channels activation is the predominant mechanism mediating URO-K10-induced pulmonary arterial relaxation. Although the highest XE991 concentration tested could not fully abolish the vasodilation induced by URO-K10, this is line with the fact that at this concentration XE991 inhibited but did not totally suppress $K_V7.4$ and $K_V7.5$ currents in HEK293 cells [29]. On the other hand, we cannot totally rule out that, in the presence of XE991, URO-K10 might activate other mechanisms such as BK_{Ca} channels as reported for other

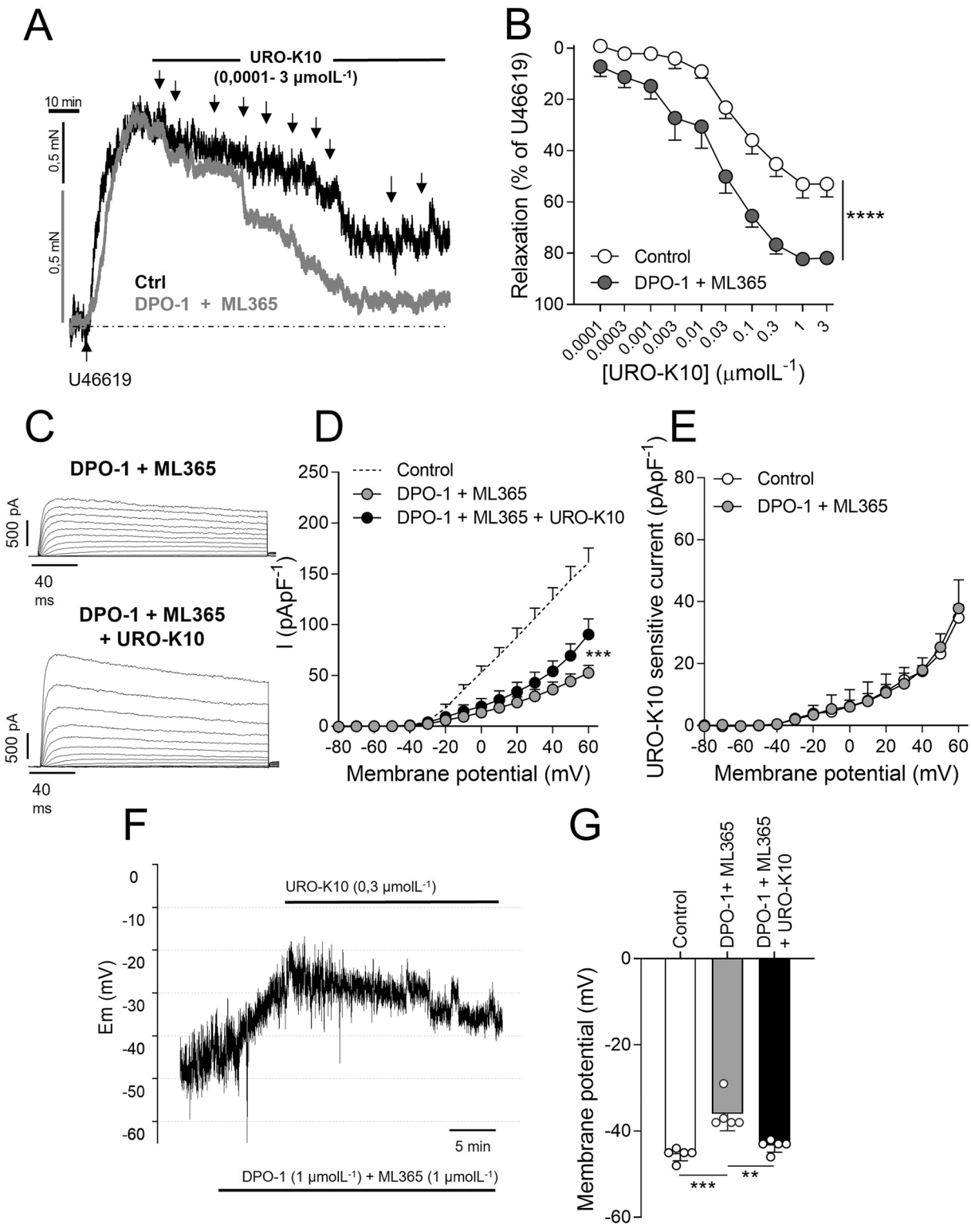

Fig. 7. . Enhanced pulmonary vascular effects of URO-K10 upon blockade of $K_V1.5$ and TASK-1 channels. URO-K10 effects were tested in rat PA incubated with the inhibitors of $K_v1.5$ and TASK-1 channels, DPO-1 and ML365 respectively, to mimic the ionic remodeling that occurs in PAH. (a) Representative original recordings and (b) averaged values of the concentration-dependent relaxation induced by URO-K10 (0.0001 – 3 μmol L^{-1}) in PA contracted with U46619 (0.1 μmol L^{-1}) in the absence (Control) and in the presence of ML365 +DPO-1 (both at 1 μmol L^{-1}) (**** $P < 0.0001$ *vs* control, n = 5, two-way ANOVA). (c) Representative K^+ current traces and (d) K^+ current-voltage relationships showing the effect of URO-K10 (0.3 μmol L^{-1}) in the presence of ML365 + DPO-1 (n = 5, *** $P < 0.001$ *vs* control, two-way ANOVA). The dashed line represents the current-voltage relationship under control conditions as a reference. (e) URO-K10-sensitive current under control conditions taken from Fig. 2 F and in presence ML365 + DPO-1 calculated from data on panel d (n = 5 and n = 6, $P > 0.05$, two-way ANOVA). (f - g) Representative recordings (f) and mean values (g) of the repolarizing effect of URO-K10 in the presence of ML365 + DPO-1 on freshly isolated PASMC. Points represent mean ± SEM of n = 5. Significant differences from controls were analyzed by paired *t*-test, * * $P < 0.01$ and * * $P < 0.001$, respectively *vs* control.

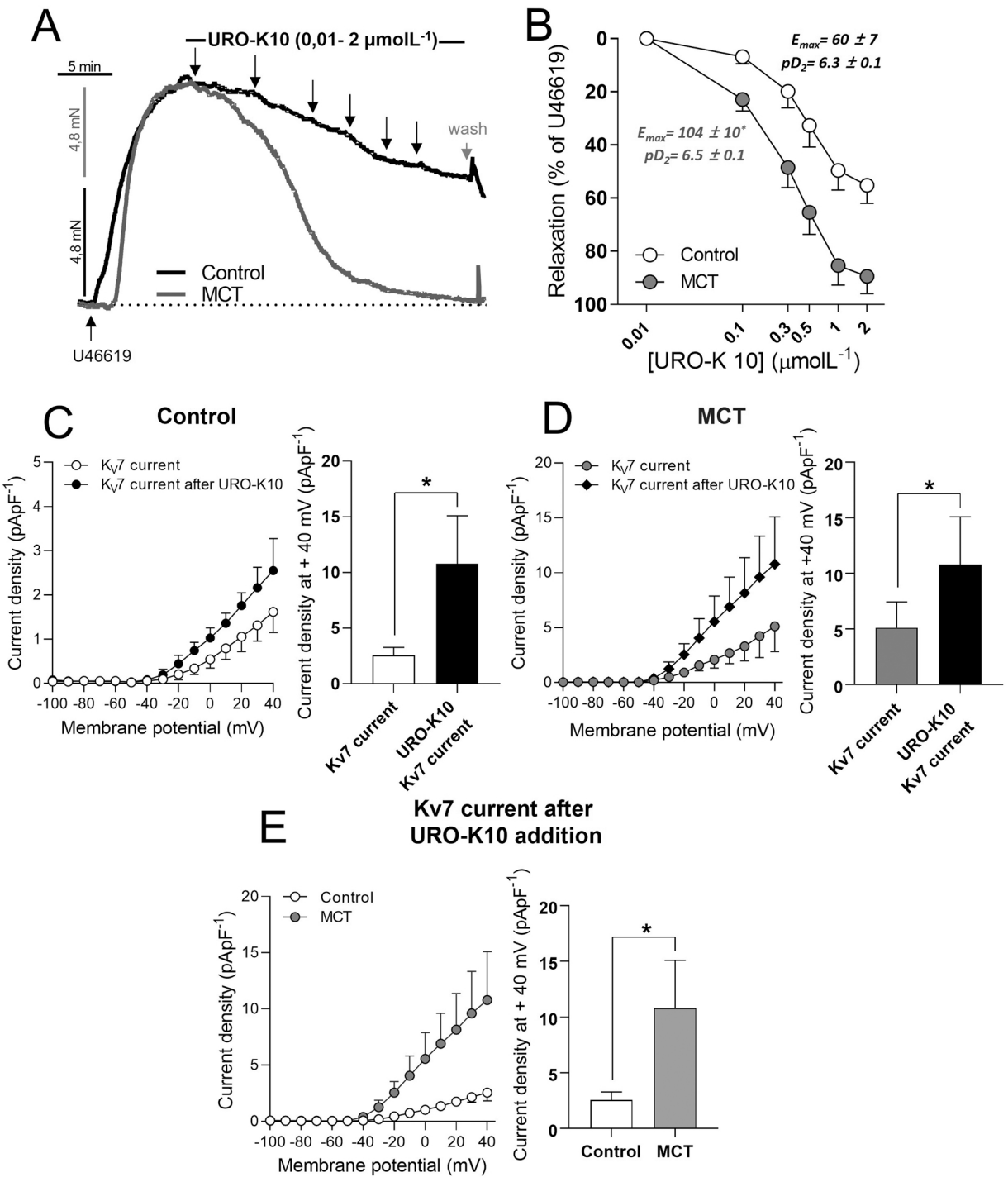

Fig. 8. . Enhanced response to URO-K10 in PA from MCT-induced PH animals. (a) Original recordings and (b) averaged values of the concentration-dependent relaxation to URO-K10 (0.0001 – 3 µmol L^{-1}) in PA from control and MCT-PH rats. Points represent mean ± SEM of 12 arteries from n = 3 animals (control group) and 10 arteries from n = 3 animals (MCT-group) ($P < 0.05$, unpaired nested *t*-test *vs* Control). (c - d) Current-voltage relationships (left panel) and inset of current density at + 40 mV (right panel) obtained after applying depolarizing ramp pulses from − 100 mV to + 40 mV for 3 s. These data show the effects of URO-K10 (1 µmol L^{-1}) on K_V7 currents in freshly isolated PASMC from control (c) or MCT-PH (d) rats. The K_V7 current and the K_V7 current after URO-K10 represent the XE991 (30 µmol L^{-1})-sensitive current in the absence and in the presence of URO-K10, respectively. (e) Current-voltage relationships (left panel) and inset of current density at + 40 mV (right panel) of K_V7 current after URO-K10 in PASMC from control or MCT-PH rats. Data were analyzed using a nested analysis at + 40 mV current, * $P < 0.05$ *vs* K_v7 current or *vs* Control. Points represent mean ± SEM of 6 cells from n = 3 (control group) and 8 cells from n = 3 (MCT-group).

compounds under these conditions [65]. However, the facts that in the presence of XE991 both, URO-K10 sensitive current was abolished, and relaxation was similar to that induced by vehicle, indicate that activation of K_V7 channels represents the main mechanism action of the drug. In line with these data, patch-clamp experiments in isolated rat PASMC revealed that URO-K10 increased the amplitude of K_V7 currents at test potentials positive to − 30 mV. In fact, the drug did not alter resting membrane potential ranging from − 51 to − 44 mV, which suggests a negligible effect of the drug under basal conditions. On the contrary, when PASMC are depolarized, as following stimulation with a

vasoconstrictor, a very clear repolarizing effect was observed.

Of note, URO-K10 exerted a much more potent and efficient pulmonary vasodilation compared to retigabine and flupirtine (present study), as well as to other K_V7 activators [5,27]. Similarly, Lee et al. showed a much greater efficacy of URO-K10 in increasing $K_V7.4$ currents than that of the $K_V7.2$–7.5 enhancer mL-213 [29]. Importantly, the K^+ channel activation and the stronger pulmonary vasodilatory effects of URO-K10 compared to retigabine were reproduced in human tissues. The vasodilator effect of URO-K10 on human pulmonary arteries was inhibited by XE991. However, unlike what was shown in rat PASMC, we were unable to confirm the nature of the outward current induced by this drug in human PASMC due to limitation of human tissue. Likewise, we found that URO-K10 had antiproliferative effects that, in contrast to retigabine [5], are evident in human PASMC from control patients. Taken together, these data indicate that URO-K10 is a novel K_V7 channel opener with pronounced vasodilator and antiproliferative effects on pulmonary vessels. Our preliminary data suggest that the antiproliferative effect of URO-K10 is attenuated in the presence of XE991. However, these data should be viewed with some caution due to limited number of samples in this set of experiments and second since this drug *per se* attenuated the BrdU signal and there is evidence that K_V7 channel blockers may also affect cell viability [66].

The marked pulmonary vascular effects of URO-K10 suggest a particular profile compared with most available K_V7 enhancers. In this regard, retigabine and other K_V7 activators with stark structural diversity are considered pore-targeted K_V7 activators as they interact with a conserved tryptophan residue in the channel pore domain through a carbonyl oxygen present in their structures [67–70]. A carbonyl oxygen is also present in URO-K10 structure and using point mutations experiments Seefeld MA et al., suggested that the drug (Compound 25 in their study) also binds the Tryptophan residue common in $K_V7.2$- $K_V7.5$ channels [28]. To try to explain the higher activity of URO-K10 in comparison with retigabine and flupirtine we focused on the potential involvement of the auxiliary subunit KCNE4. In fact, this subunit was reported to enhance $K_V7.4$ channel activity [25] and to contribute to vasodilation induced by retigabine and S-1 [26]. Accordingly, we found that KCNE4 deletion attenuated retigabine and flupirtine-induced vasodilation. In contrast, KCNE4 deletion did not affect URO-K10-induced relaxation. This result agrees with the study by Lee et al. who found that, KCNE4 was not required for URO-K10 to alter the voltage-sensitivity of Kv7.4 or Kv7.5 and was actually inhibitory for the effect of this agent on channel conductance [29]. Our data indicates that the presence of KCNE4 is relevant for retigabine and flupirtine, but not for URO-K10-mediated, pulmonary vascular effects.

Since PAH is associated with downregulation of several K^+ channels (especially $K_V1.5$ and TASK-1 channels) [15,37,52–58,71] we next decided to test the effects of URO-K10 in the presence of inhibitors of $K_V1.5$ and TASK-1 channels mimicking the ionic remodelling characteristic of the disease. Using this approach, we previously found that following inhibition of these channels retigabine-induced K^+ currents, hyperpolarization and vasodilation were markedly enhanced [5]. We also found a higher KCNE4 membrane abundance and suggested a potential role of this subunit in the enhanced effects of retigabine. Herein we found that URO-K10-mediated pulmonary relaxation was enhanced in the presence of $K_V1.5$ and TASK-1 inhibitors. Nevertheless URO-K10-sensitive K^+ current was comparable to that recorded under control conditions. Thus, it is tempting to speculate that the presence of KCNE4 in the plasma membrane may contribute to the electrophysiological and vascular effects of retigabine and related compounds but not to those of URO-K10. Although we do not yet know the precise reason for the increased hyperpolarization and relaxation of URO-K10, it is likely that the drug is most effective when more depolarized membrane potentials are reached, close to the voltage threshold of K_V7 channel activation, as occurs in the presence of $K_V1.5$ and TASK-1 inhibitors.

KCNE4 not only regulates the activity but also the expression of K_V7 channels. Thus, KCNE4 overexpression reduced $K_V7.4$ expression in heterologous systems [51] but, on the other hand, increased the membrane abundance of $K_V7.4$ [25], and knockdown of KCNE4 by morpholino treatment reduced $K_V7.4$ in the cell membrane of arterial smooth muscle cells [25]. Moreover, $K_V7.4$ protein expression is markedly downregulated in mesenteric arteries from male *KCNE4* KO mice [26]. In line with this data, we found that KCNE4 deletion was associated with reduced total $K_V7.4$ protein expression. Intriguingly, the downregulation of $K_V7.4$ observed in morpholino KCNE4-targeted arteries did not affect URO-K10-induced relaxation. This was unexpected since $K_V7.4$ channels are activated by URO-K10 [29] and are considered main contributors of the K_V7 channel family in the vasculature. However, we should take under consideration that $K_V7.5$ protein expression is not affected by KCNE4 deletion and that URO-K10 activates also, although to a lesser extent, $K_V7.3$ and $K_V7.5$ channels [28]. Therefore, it is possible that activation of other K_V7 channels may compensate the small decrease in $K_V7.4$ expression (by a 25%) thus, maintaining URO-K10-induced relaxation in morpholino KCNE4-targeted arteries. In line with this, there are some examples showing that downregulation of $K_V7.4$ channels does not affect relaxation of some K_V7 channel agonists. For instance, vasodilation of mesenteric arteries to mL-213 was not affected in female *KCNE4* KO mice despite clear $K_V7.4$ downregulation [26].

The impairment of the NO/cGMP and the PGI_2 signalling pathway is a hallmark in PAH [10,72,73] and current PAH treatments such as sildenafil, riociguat and selexipag rely on the stimulation of the NO/cGMP pathway and on the prostacyclin receptor activation, respectively. Of note, K_V7 channel activation contributes to riociguat- and sildenafil-induced pulmonary vasodilation [4,7] and has also been recently implicated in the selexipag-mediated vasodilation [74]. Interestingly, evidence from different experimental models suggests that pulmonary vasodilation due to the NO/cGMP pathway is attenuated in PH [18–21] while the responses to K_V7 agonists are even improved [5]. Herein we observed a similar behaviour for URO-K10, but noteworthy, this novel K_V7 agonist can achieve a full vasodilation of these diseased arteries. Likewise, URO-K10-induced K^+ currents were markedly augmented in PASMC from PH animals compared to those from healthy animals.

5. Conclusions

Our results indicate that URO-K10 is a KCNE4-independent K_V7 channel activator with increased pulmonary vascular effects compared to classical K_V7 channel activators. The increasing development of new K_V7 modulators with potential improved profiles, such as that observed in our study with URO-K10, suggests that this group of drugs may represent a promising strategy for a variety of clinical applications such as PAH.

CRediT authorship contribution statement

Conceptualization, A.C. and B.C.; formal analysis, A.V.-Z., B.C., B.B., G.T., J.N.-D., D.M-C, J.W., M.V.-E., and S.C.; investigation, A.V.-Z., B.B., G.T., J.N.-D., D.M-C, J.W., M.V.-E. and S.C.; resources, B.D.O.N.; writing—original draft preparation, A.C. and B.C.; writing—review and editing, A.C., A.V.-Z., B.C., F.P.-V., I.G., J.N.-D., L.M. and S.J.K.; project administration, B.B.; funding acquisition, A.C. and B.C. All authors have read and agreed to the published version of the manuscript.

Declaration of Competing Interest

None. The authors have reported that they have no relationships with industry relevant to the contents of this paper to disclose. The funders played no role in the study design; nor in the collection, analyses, interpretation of data, nor in the writing of the manuscript.

Data availability

Data will be made available on request.

Acknowledgements

The authors thank the support provided by the animal facility unit of the Medicine Faculty, Complutense University of Madrid.

Institutional review board statement

The study was conducted according to the guidelines of the Declaration of Helsinki, and approved by the Institutional Review Boards of Universidad Complutense and Hospital de Getafe, Madrid, Spain.

Informed consent statement

Verbal informed consent was obtained from all subjects involved in the study whose lung tissue was discarded by pathologists following thoracic surgery.

Declaration of transparency and scientific rigour

This Declaration acknowledges that this paper adheres to the principles for transparent reporting and scientific rigour of preclinical research as stated in the BJP guidelines for Natural Products Research, Design and Analysis, Immunoblotting and Immunochemistry, and Animal Experimentation, and as recommended by funding agencies, publishers and other organizations engaged with supporting research.

Funding statement

This work was funded by grants from the Spanish Ministry of Science and Innovation (PID2020-117939RB-I00 to A.C. and PID2019-107363RB-I00 to F.P.V.), and Instituto de Salud Carlos III (PI19/01616 to L.M.) with funds from the European Union (Fondo Europeo de Desarrollo Regional FEDER), by Korea National Research Foundation (NRF 2021R1A2C2007243 to S.J.K.) and Fundación Contra la Hipertensión Pulmonar-EMPATHY. M.V-E. was supported by UCM and FPU fellowships.

Appendix A. Supporting information

Supplementary data associated with this article can be found in the online version at doi:10.1016/j.biopha.2023.114952.

References

[1] J.M. Haick, K.L. Byron, Novel treatment strategies for smooth muscle disorders: Targeting Kv7 potassium channels, Pharmacol. Ther. 165 (2016) 14–25, https://doi.org/10.1016/j.pharmthera.2016.05.002.
[2] A.R. Mackie, K.L. Byron, Cardiovascular KCNQ (Kv7) potassium channels: Physiological regulators and new targets for therapeutic intervention, Mol. Pharm. 74 (2008) 1171–1179, https://doi.org/10.1124/mol.108.049825.
[3] V. Barrese, J.B. Stott, I.A. Greenwood, KCNQ-encoded potassium channels as therapeutic targets, Annu. Rev. Pharmacol. Toxicol. 58 (2018) 625–673, https://doi.org/10.1146/annurev-pharmtox.
[4] G. Mondéjar-Parreño, J. Moral-Sanz, B. Barreira, A. de la Cruz, T. Gonzalez, M. Callejo, S. Esquivel-Ruiz, D. Morales-Cano, L. Moreno, C. Valenzuela, F. Perez-Vizcaino, A. Cogolludo, Activation of Kv7 channels as a novel mechanism for NO/cGMP-induced pulmonary vasodilation, Br. J. Pharm. 176 (2019) 2131–2145, https://doi.org/10.1111/bph.14662.
[5] G. Mondéjar-Parreño, B. Barreira, M. Callejo, D. Morales-Cano, V. Barrese, S. Esquivel-Ruiz, M.A. Olivencia, M. Macías, L. Moreno, I.A. Greenwood, F. Perez-Vizcaino, A. Cogolludo, Uncovered contribution of Kv7 channels to pulmonary vascular tone in pulmonary arterial hypertension, Hypertension (2020) 1134–1146, https://doi.org/10.1161/HYPERTENSIONAHA.120.15221.
[6] S. Joshi, V. Sedivy, D. Hodyc, J. Herget, A.M. Gurney, KCNQ modulators reveal a key role for KCNQ potassium channels in regulating the tone of rat pulmonary artery smooth muscle, J. Pharmacol. Exp. Ther. 329 (2009) 368, https://doi.org/10.1124/jpet.108.147785.
[7] M. Al-chawishly, O. Loveland, A.M. Gurney, Kv7 channels in cyclic-nucleotide dependent relaxation of rat intra-pulmonary artery, Biomolecules 12 (2022), https://doi.org/10.3390/biom12030429.
[8] K.W. Prins, T. Thenappan, World Health Organization Group I pulmonary hypertension: epidemiology and pathophysiology, Cardiol. Clin. 34 (2016) 363–374, https://doi.org/10.1016/j.ccl.2016.04.001.
[9] M. Humbert, G. Kovacs, M.M. Hoeper, R. Badagliacca, R.M.F. Berger, M. Brida, J. Carlsen, A.J.S. Coats, P. Escribano-Subias, P. Ferrari, D.S. Ferreira, H. A. Ghofrani, G. Giannakoulas, D.G. Kiely, E. Mayer, G. Meszaros, B. Nagavci, K. M. Olsson, J. Pepke-Zaba, J.K. Quint, G. Rådegran, G. Simonneau, O. Sitbon, T. Tonia, M. Toshner, J.L. Vachiery, A. Vonk Noordegraaf, M. Delcroix, S. Rosenkranz, M. Schwerzmann, A.T. Dinh-Xuan, A. Bush, M. Abdelhamid, V. Aboyans, E. Arbustini, R. Asteggiano, J.A. Barberà, M. Beghetti, J. Čelutkienė, M. Cikes, R. Condliffe, F. de Man, V. Falk, L. Fauchier, S. Gaine, N. Galié, W. Gin-Sing, J. Granton, E. Grünig, P.M. Hassoun, M. Hellemons, T. Jaarsma, B. Kjellström, F.A. Klok, A. Konradi, K.C. Koskinas, D. Kotecha, I. Lang, B.S. Lewis, A. Linhart, G. Y.H. Lip, M.L. Løchen, A.G. Mathioudakis, R. Mindham, S. Moledina, R. Naeije, J. C. Nielsen, H. Olschewski, I. Opitz, S.E. Petersen, E. Prescott, A. Rakisheva, A. Reis, A.D. Ristić, N. Roche, R. Rodrigues, C. Selton-Suty, R. Souza, A.J. Swift, R. M. Touyz, S. Ulrich, M.R. Wilkins, S.J. Wort, 2022 ESC/ERS Guidelines for the diagnosis and treatment of pulmonary hypertension, Eur. Heart J. 43 (2022) 3618–3731, https://doi.org/10.1093/eurheartj/ehac237.
[10] R.T. Schermuly, H.A. Ghofrani, M.R. Wilkins, F. Grimminger, Mechanisms of disease: Pulmonary arterial hypertension, Nat. Rev. Cardiol. 8 (2011) 443–455, https://doi.org/10.1038/nrcardio.2011.87.
[11] E.D. Burg, C. v Remillard, J.X.J. Yuan, Potassium channels in the regulation of pulmonary artery smooth muscle cell proliferation and apoptosis: Pharmacotherapeutic implications, in: Br J Pharmacol, 2008, https://doi.org/10.1038/sj.bjp.0707635.
[12] A. Cogolludo, L. Moreno, E. Villamor, Mechanisms controlling vascular tone in pulmonary arterial hypertension: Implications for vasodilator therapy, Pharmacology 79 (2007) 65–75, https://doi.org/10.1159/000097754.
[13] L.A. Shimoda, D.J. Manalo, J.S.K. Sham, G.L. Semenza, J.T. Sylvester, Partial HIF-1 deficiency impairs pulmonary arterial myocyte electrophysiological responses to hypoxia, Am. J. Physiol. Lung Cell Mol. Physiol. 281 (2001) L202–L208. ⟨https://journals.physiology.org/doi/full/10.1152/ajplung.2001.281.1.L202⟩.
[14] J. Wang, L. Weigand, W. Wang, J.T. Sylvester, L.A. Shimoda, Chronic hypoxia inhibits Kv channel gene expression in rat distal pulmonary artery, Am. J. Physiol. Lung Cell Mol. Physiol. 288 (2005) 1049–1058, https://doi.org/10.1152/ajplung.00379.2004.-In.
[15] J. Xiao-Jian Yuan, A.M. Aldinger, M. Juhaszova, J. Wang, J.V. Conte, S.P. Gaine, J. B. Orens, L.J. Rubin, Dysfunctional voltage-gated K channels in pulmonary artery smooth muscle cells of patients with primary pulmonary hypertension (https://doi.org/https://), Circulation 98 (1998) 1400–1406, https://doi.org/10.1161/01.cir.98.14.1400.
[16] I. Morecroft, A. Murray, M. Nilsen, A.M. Gurney, M.R. MacLean, Treatment with the Kv7 potassium channel activator flupirtine is beneficial in two independent mouse models of pulmonary hypertension, Br. J. Pharm. 157 (2009) 1241–1249, https://doi.org/10.1111/j.1476-5381.2009.00283.x.
[17] V. Sedivy, S. Joshi, Y. Ghaly, R. Mizera, M. Zaloudikova, S. Brennan, J. Novotna, J. Herget, A.M. Gurney, Role of Kv7 channels in responses of the pulmonary circulation to hypoxia, Am. J. Physiol. Lung Cell Mol. Physiol. 308 (2015) 48–57, https://doi.org/10.1152/ajplung.00362.2013.-Hypoxic.
[18] A.S. Sikarwar, M. Hinton, K.T. Santhosh, P. Dhanaraj, M. Talabis, P. Chelikani, S. Dakshinamurti, Hypoxia inhibits adenylyl cyclase catalytic activity in a porcine model of persistent pulmonary hypertension of the newborn, Am. J. Physiol. Lung Cell Mol. Physiol. 315 (2018) 933–944, https://doi.org/10.1152/ajplung.00130.2018.-Persistent.
[19] V. Mam, A.F. Tanbe, S.H. Vitali, E. Arons, H.A. Christou, R.A. Khalil, Impaired vasoconstriction and nitric oxide-mediated relaxation in pulmonary arteries of hypoxia- and monocrotaline-induced pulmonary hypertensive rats, J. Pharmacol. Exp. Ther. 332 (2010) 455, https://doi.org/10.1124/jpet.109.160119.
[20] H. Christou, H. Hudalla, Z. Michael, E.J. Filatava, J. Li, M. Zhu, J.S. Possomato-Vieira, C. Dias-Junior, S. Kourembanas, R.A. Khalil, Impaired pulmonary arterial vasoconstriction and nitric oxide–mediated relaxation underlie severe pulmonary hypertension in the sugen-hypoxia rat model, J. Pharm. Exp. Ther. 364 (2018) 258–274, https://doi.org/10.1124/jpet.117.244798.
[21] J. Milara, J. Escrivá, J. Luis Ortiz, G. Juan, E. Artigues, E. Morcillo, J. Cortijo, Vascular effects of sildenafil in patients with pulmonary fibrosis and pulmonary hypertension: an ex vivo/in vitro study, Eur. Respir. J. 47 (2016) 1737–1749, https://doi.org/10.1183/13993003.01259-2015.
[22] G. Mondejar-Parreño, F. Perez-Vizcaino, A. Cogolludo, Kv7 channels in lung diseases, Front Physiol. 11 (2020) 634, https://doi.org/10.3389/fphys.2020.00634.
[23] G. Abbott, KCNQs: ligand- and voltage-gated potassium channels, Front Physiol. 11 (2020), https://doi.org/10.3389/fphys.2020.00583.
[24] K.L. Byron, L.I. Brueggemann, Kv7 potassium channels as signal transduction intermediates in the control of microvascular tone, Microcirculation 25 (2018), https://doi.org/10.1111/micc.12419.
[25] T. Jepps, G. Carr, P. Lundegaard, S.P. Olesen, I. Greenwood, Fundamental role for the KCNE4 ancillary subunit in Kv7.4 regulation of arterial tone, J. Physiol. 593 (2015) 5325–5340, https://doi.org/10.1113/JP271286.
[26] G. Abbott, T. Jepps, KCNE4 deletion sex-dependently alters vascular reactivity, J. Vasc. Res 53 (2016) 138–148, https://doi.org/10.1159/000449060.
[27] D. Morales-Cano, B. Barreira, B. De Olaiz Navarro, M. Callejo, G. Mondejar-Parreño, S. Esquivel-Ruiz, J.A. Lorente, L. Moreno, J.A. Barberá, Á. Cogolludo,

F. Perez-Vizcaino, Oxygen-sensitivity and pulmonary selectivity of vasodilators as potential drugs for pulmonary hypertension, Antioxidants 10 (2021) 155, https://doi.org/10.3390/antiox10020155.
[28] M.A. Seefeld, H. Lin, J. Holenz, D. Downie, B. Donovan, T. Fu, K. Pasikanti, W. Zhen, M. Cato, K.W. Chaudhary, P. Brady, T. Bakshi, D. Morrow, S. Rajagopal, S.K. Samanta, N. Madhyastha, B.M. Kuppusamy, R.W. Dougherty, R. Bhamidipati, Z. Mohd, G.A. Higgins, M. Chapman, C. Rouget, P. Lluel, Y. Matsuoka, Novel KV7 ion channel openers for the treatment of epilepsy and implications for detrusor tissue contraction, Bioorg. Med Chem. Lett. 28 (2018) 3793–3797, https://doi.org/10.1016/j.bmcl.2018.09.036.
[29] J.E. Lee, C.H. Park, H. Kang, J. Ko, S. Cho, J. Woo, M.R. Chae, S.W. Lee, S.J. Kim, J. Kim, I. So, The agonistic action of URO-K10 on Kv7.4 and 7.5 channels is attenuated by co-expression of KCNE4 ancillary subunit, Korean J. Physiol. Pharmacol. 24 (2020) 503–516, https://doi.org/10.4196/kjpp.2020.24.6.503.
[30] R. Pandolfi, B. Barreira, E. Moreno, V. Lara-Acedo, D. Morales-Cano, A. Martínez-Ramas, B. de Olaiz Navarro, R. Herrero, J.Á. Lorente, Á. Cogolludo, F. Pérez-Vizcaíno, L. Moreno, Role of acid sphingomyelinase and IL-6 as mediators of endotoxin-induced pulmonary vascular dysfunction, Thorax 72 (2017) 460–471, https://doi.org/10.1136/thoraxjnl-2015-208067.
[31] A. Cogolludo, L. Moreno, G. Frazziano, J. Moral-Sanz, C. Menendez, J. Castañeda, C. González, E. Villamor, F. Perez-Vizcaino, Activation of neutral sphingomyelinase is involved in acute hypoxic pulmonary vasoconstriction, Cardiovasc Res 82 (2009) 296–302, https://doi.org/10.1093/cvr/cvn349.
[32] M.J. Mulvany, W. Halpern, Contractile properties of small arterial resistance vessels in spontaneously hypertensive and normotensive rats, Circ. Res 41 (1997) 19–26, https://doi.org/10.1161/01.res.41.1.19.
[33] M. Ozaki, C. Marshall, Y. Amaki, B.E. Marshall, C. Ozaki, Y. Marshall, B.E. M. Amaki, Role of wall tension in hypoxic responses of isolated rat pulmonary arteries (https://doi.org/DOI:), Lung Cell. Mol. Physiol. 19 (1998) 1069–1077, https://doi.org/10.1152/ajplung.1998.275.6.L1069.
[34] A. Cogolludo, L. Moreno, G. Frazziano, J. Moral-Sanz, C. Menendez, J. Castañeda, C. González, E. Villamor, F. Perez-Vizcaino, Activation of neutral sphingomyelinase is involved in acute hypoxic pulmonary vasoconstriction, Cardiovasc. Res. 82 (2009) 296–302, https://doi.org/10.1093/cvr/cvn349.
[35] F. Pérez-Vizcaino, E. Villamor, J. Duarte, J. Tamargo, Involvement of protein kinase C in reduced relaxant responses to the NO/cyclic GMP pathway in piglet pulmonary arteries contracted by the thromboxane A 2-mimetic U46619 1, Br. J. Pharm. 121 (1997) 1323–1333, https://doi.org/10.1038/sj.bjp.0701257.
[36] F. Pérez-Vizcaíno, E. Villamor, B. Fernandez del Pozo, M. Moro, J. Tamargo, Lack of endotoxin-induced hyporesponsiveness to U46619 in isolated neonatal porcine pulmonary but not mesenteric arteries, J. Vasc. Res 33 (1996) 249–257, https://doi.org/10.1159/000159152.
[37] D. Morales-Cano, C. Menendez, E. Moreno, J. Moral-Sanz, B. Barreira, P. Galindo, R. Pandolfi, R. Jimenez, L. Moreno, A. Cogolludo, J. Duarte, F. Perez-Vizcaino, The flavonoid quercetin reverses pulmonary hypertension in rats, PLoS One 9 (2014), e114492, https://doi.org/10.1371/journal.pone.0114492.
[38] A. Cogolludo, L. Moreno, F. Lodi, G. Frazziano, L. Cobeño, J. Tamargo, F. Perez-Vizcaino, Serotonin inhibits voltage-gated K+ currents in pulmonary artery smooth muscle cells: Role of 5-HT2A receptors, caveolin-1, and KV1.5 channel internalization, Circ. Res 98 (2006) 931–938, https://doi.org/10.1161/01.RES.0000216858.04599.e1.
[39] G. Mondejar-Parreño, D. Morales-Cano, B. Barreira, M. Callejo, J. Ruiz-Cabello, L. Moreno, S. Esquivel-Ruiz, A. Mathie, G. Butrous, F. Perez-Vizcaino, A. Cogolludo, HIV transgene expression impairs K channel function in the pulmonary vasculature, Am. J. Physiol. Lung Cell Mol. Physiol. 315 (2018) 711–723, https://doi.org/10.1152/ajplung.00045.2018.-Human.
[40] D. Morales-Cano, L. Moreno, B. Barreira, R. Pandolfi, V. Chamorro, R. Jimenez, E. Villamor, J. Duarte, F. Perez-Vizcaino, A. Cogolludo, Kv7 channels critically determine coronary artery reactivity: Left-right differences and down-regulation by hyperglycaemia, Cardiovasc Res 106 (2015) 98–108, https://doi.org/10.1093/cvr/cvv020.
[41] J.E. Summerton, Morpholino, siRNA, and S-DNA compared: impact of structure and mechanism of action on off-target effects and sequence specificity, Curr. Top. Med Chem. 7 (2007) 651–660, https://doi.org/10.2174/156802607780487740.
[42] J. Summerton, Morpholino antisense oligomers: the case for an RNase H-independent structural type, Biochim. Et. Biophys. Acta 1489 (1999) 141–158, https://doi.org/10.1016/s0167-4781(99)00150-5.
[43] G. Mondejar-Parreño, M. Callejo, B. Barreira, D. Morales-Cano, S. Esquivel-Ruiz, L. Moreno, A. Cogolludo, F. Perez-Vizcaino, miR-1 is increased in pulmonary hypertension and downregulates Kv1.5 channels in rat pulmonary arteries. J. Physiol. 597 (2019) 1185–1197, https://doi.org/10.1113/JP276054.
[44] A. Vera-Zambrano, M. Baena-Nuevo, S. Rinné, M. Villegas-Esguevillas, B. Barreira, G. Telli, A. de Benito-Bueno, J.A. Blázquez, B. Climent, F. Pérez-Vizcaino, C. Valenzuela, N. Decher, T. Gonzalez, A. Cogolludo, Sigma-1 receptor modulation fine-tunes KV1.5 channels and impacts pulmonary vascular function. Pharm. Res. 189 (2023), 106684 https://doi.org/10.1016/j.phrs.2023.106684.
[45] B. Manoury, S.L. Etheridge, J. Reid, A.M. Gurney, Organ culture mimics the effects of hypoxia on membrane potential, K(+) channels and vessel tone in pulmonary artery, Br. J. Pharm. 158 (2009) 848–861, https://doi.org/10.1111/j.1476-5381.2009.00353.x.
[46] B. Climent, E. Santiago, A. Sánchez, M. Muñoz-Picos, F. Pérez–Vizcaíno, A. García-Sacristán, L. Rivera, D. Prieto, Metabolic syndrome inhibits store-operated Ca2+ entry and calcium-induced calcium-release mechanism in coronary artery smooth muscle, Biochem Pharm. 182 (2020), https://doi.org/10.1016/j.bcp.2020.114222.
[47] S.P.H. Alexander, R.E. Roberts, B.R.S. Broughton, C.G. Sobey, C.H. George, S. C. Stanford, G. Cirino, J.R. Docherty, M.A. Giembycz, D. Hoyer, P.A. Insel, A. A. Izzo, Y. Ji, D.J. MacEwan, J. Mangum, S. Wonnacott, A. Ahluwalia, Goals and practicalities of immunoblotting and immunohistochemistry: A guide for submission to the British Journal of Pharmacology. Br. J. Pharmacol. 175 (2018) 407–411, https://doi.org/10.1111/bph.14112.
[48] J.B. Stott, V. Barrese, T.A. Jepps, E.V. Leighton, I.A. Greenwood, Contribution of Kv7 channels to natriuretic peptide mediated vasodilation in normal and hypertensive rats, Hypertension 65 (2015) 676–682, https://doi.org/10.1161/HYPERTENSIONAHA.114.04373.
[49] D. Morales-Cano, L. Moreno, B. Barreira, R. Pandolfi, V. Chamorro, R. Jimenez, E. Villamor, J. Duarte, F. Perez-Vizcaino, A. Cogolludo, Kv7 channels critically determine coronary artery reactivity: left-right differences and down-regulation by hyperglycaemia, Cardiovasc Res 106 (2015) 98–108, https://doi.org/10.1093/cvr/cvv020.
[50] C. Serrano-Novillo, A. Oliveras, J.C. Ferreres, E. Condom, A. Felipe, Remodeling of Kv7.1 and Kv7.5 Expression in Vascular Tumors. Int J. Mol. Sci. 21 (2020) https://doi.org/10.3390/ijms21176019.
[51] N. Strutz-Seebohm, G. Seebohm, O. Fedorenko, R. Baltaev, J. Engel, M. Knirsch, F. Lang, Functional coassembly of KCNQ4 with KCNE-β-subunits in xenopus oocytes, Cell Physiol. Biochem 18 (2006) 57–66, https://doi.org/10.1159/000095158.
[52] G. Mondejar-Parreño, M. Callejo, B. Barreira, D. Morales-Cano, S. Esquivel-Ruiz, M. Filice, L. Moreno, A. Cogolludo, F. Perez-Vizcaino, miR-1 induces endothelial dysfunction in rat pulmonary arteries, J. Physiol. Biochem 75 (2019) 519–529, https://doi.org/10.1007/s13105-019-00696-2/Published.
[53] M. Lambert, A. Boet, C. Rucker-Martin, P. Mendes-Ferreira, V. Capuano, S. Hatem, R. Adão, C. Brás-Silva, A. Hautefort, J.B. Michel, P. Dorfmuller, E. Fadel, T. Kotsimbos, L. Price, P. Jourdon, D. Montani, M. Humbert, F. Perros, F. Antigny, Loss of KCNK3 is a hallmark of RV hypertrophy/dysfunction associated with pulmonary hypertension, Cardiovasc Res 114 (2018) 880–893, https://doi.org/10.1093/cvr/cvy016.
[54] J. Wang, M. Juhaszova, L.J. Rubin, X.-J. Yuan, Hypoxia inhibits gene expression of voltage-gated K1 channel a subunits inpulmonary artery smooth muscle cells, J. Clin. Invest. 100 (1997) 2347–2353, https://doi.org/https://10.1172/JCI119774.
[55] A.M. Gurney, O.N. Osipenko, D. MacMillan, K.M. McFarlane, R.J. Tate, F.E. J. Kempsill, Two-pore domain K channel, TASK-1, in pulmonary artery smooth muscle cells, Circ. Res 93 (2003) 957–964, https://doi.org/10.1161/01.RES.0000099883.68414.61.
[56] X.-J. Yuan, J. Wang, M. Juhaszova, V.A. Golovina, L.J. Rubin, Molecular basis and function of voltage-gated K channels in pulmonary arterial smooth muscle cells (https://doi.org/https://), Am. J. Physiol. 274 (1998) L621–L635, https://doi.org/10.1152/ajplung.1998.274.4.L621.
[57] A. Olschewski, E.L. Veale, B.M. Nagy, C. Nagaraj, G. Kwapiszewska, F. Antigny, M. Lambert, M. Humbert, G. Czirják, P. Enyedi, A. Mathie, TASK-1 (KCNK3) channels in the lung: From cell biology to clinical implications, Eur. Respir. J. 50 (2017), https://doi.org/10.1183/13993003.00754-2017.
[58] F. Antigny, A. Hautefort, J. Meloche, M. Belacel-Ouari, B. Manoury, C. Rucker-Martin, C. Péchoux, F. Potus, V. Nadeau, E. Tremblay, G. Ruffenach, A. Bourgeois, P. Dorfmüller, S. Breuils-Bonnet, E. Fadel, B. Ranchoux, P. Jourdon, B. Girerd, D. Montani, S. Provencher, S. Bonnet, G. Simonneau, M. Humbert, F. Perros, Potassium channel subfamily K member 3 (KCNK3) contributes to the development of pulmonary arterial hypertension, Circulation 133 (2016) 1371–1385, https://doi.org/10.1161/CIRCULATIONAHA.115.020951.
[59] T.A. Jepps, S.P. Olesen, I.A. Greenwood, One man's side effect is another man's therapeutic opportunity: Targeting Kv7 channels in smooth muscle disorders, Br. J. Pharm. 168 (2013) 19–27, https://doi.org/10.1111/j.1476-5381.2012.02133.x.
[60] J.B. Stott, T.A. Jepps, I.A. Greenwood, KV7 potassium channels: A new therapeutic target in smooth muscle disorders, Drug Discov. Today 19 (2014) 413–424, https://doi.org/10.1016/j.drudis.2013.12.003.
[61] M. Borgini, P. Mondal, R. Liu, P. Wipf, Chemical modulation of Kv7 potassium channels, RSC Med. Chem. 12 (2021) 483–537, https://doi.org/10.1039/d0md00328j.
[62] N. Brickel, P. Gandhi, K. VanLandingham, J. Hammond, S. DeRossett, The urinary safety profile and secondary renal effects of retigabine (ezogabine): A first-in-class antiepileptic drug that targets KCNQ (K v 7) potassium channels, Epilepsia 53 (2012) 606–612, https://doi.org/10.1111/j.1528-1167.2012.03441.x.
[63] F. Puls, C. Agne, F. Klein, M. Koch, K. Rifai, M.P. Manns, J. Borlak, H.H. Kreipe, Pathology of flupirtine-induced liver injury: a histological and clinical study of six cases, Virchows Arch. 458 (2011) 709–716, https://doi.org/10.1007/s00428-011-1087-9.
[64] M.C. Michel, P. Radziszewski, C. Falconer, D. Marschall-Kehrel, K. Blot, Unexpected frequent hepatotoxicity of a prescription drug, flupirtine, marketed for about 30 years, Br. J. Clin. Pharm. 73 (2012) 821–825, https://doi.org/10.1111/j.1365-2125.2011.04138.x.
[65] O. Zavaritskaya, S. Dudem, D. Ma, K. Rabab, S. Albrecht, D. Tsvetkov, M. Kassmann, K. Thornbury, M. Mladenov, C. Kammermeier, G. Sergeant, N. Mullins, O. Wouappi, H. Wurm, A. Kannt, M. Gollasch, M. Hollywood, R. Schubert, Vasodilation of rat skeletal muscle arteries by the novel BK channel opener GoSlo is mediated by the simultaneous activation of BK and Kv 7 channels, Br. J. Pharm. 177 (2020) 1164–1186, https://doi.org/10.1111/bph.14910.
[66] P. Cidad, L. Jiménez-Pérez, D. García-Arribas, E. Miguel-Velado, S. Tajada, C. Ruiz-McDavitt, J.R. López-López, M.T. Pérez-García, Kv1.3 channels can modulate cell proliferation during phenotypic switch by an ion-flux independent mechanism, Arterioscler. Thromb. Vasc. Biol. 32 (2012) 1299–1307, https://doi.org/10.1161/ATVBAHA.111.242727.

[67] R.Y. Kim, M.C. Yau, J.D. Galpin, G. Seebohm, C.A. Ahern, S.A. Pless, H.T. Kurata, Atomic basis for therapeutic activation of neuronal potassium channels, Nat. Commun. 6 (2015) 8116, https://doi.org/10.1038/ncomms9116.
[68] T.V. Wuttke, G. Seebohm, S. Bail, S. Maljevic, H. Lerche, The new anticonvulsant retigabine favors voltage-dependent opening of the Kv7.2 (KCNQ2) channel by binding to its activation gate, Mol. Pharm. 67 (2005) 1009, https://doi.org/10.1124/mol.104.010793.
[69] W. Lange, J. Geißendörfer, A. Schenzer, J. Grötzinger, G. Seebohm, T. Friedrich, M. Schwake, Refinement of the binding site and mode of action of theanticonvulsant Retigabine on KCNQ K+channels, Mol. Pharm. 75 (2009) 272, https://doi.org/10.1124/mol.108.052282.
[70] A. Schenzer, T. Friedrich, M. Pusch, P. Saftig, T.J. Jentsch, J. Grötzinger, M. Schwake, Molecular determinants of KCNQ (K v 7) K channel sensitivity to the anticonvulsant retigabine, J. Neurosci. 25 (2005) 5051–5060, https://doi.org/10.1523/JNEUROSCI.0128-05.2005.
[71] M. Callejo, G. Mondejar-Parreño, D. Morales-Cano, B. Barreira, S. Esquivel-Ruiz, M. Angel Olivencia, G. Manaud, F. Perros, J. Duarte, X. Laura Moreno, A. Cogolludo, F. Perez-Vizcaíno, Vitamin D deficiency downregulates TASK-1 channels and induces pulmonary vascular dysfunction, Am. J. Physiol. Lung Cell Mol. Physiol. 319 (2020) 627–640, https://doi.org/10.1152/ajplung.00475.
[72] J.R. Klinger, P.J. Kadowitz, The nitric oxide pathway in pulmonary vascular disease, Am. J. Cardiol. 120 (2017) S71–S79, https://doi.org/10.1016/j.amjcard.2017.06.012.
[73] N. Galiè, R.N. Channick, R.P. Frantz, E. Grünig, Z.C. Jing, O. Moiseeva, I. R. Preston, T. Pulido, Z. Safdar, Y. Tamura, V.V. McLaughlin, Risk stratification and medical therapy of pulmonary arterial hypertension, Eur. Respir. J. 53 (2019), https://doi.org/10.1183/13993003.01889-2018.
[74] S.N. Baldwin, E.A. Forrester, L. McEwan, I.A. Greenwood, Sexual dimorphism in prostacyclin-mimetic responses within rat mesenteric arteries: A novel role for KV 7.1 in shaping IP receptor-mediated relaxation, Br. J. Pharm. 179 (2022) 1338–1352, https://doi.org/10.1111/bph.15722.